ผลกระทบของทิศทางการเทต่อกำลังเฉือนทะลุของแผ่นพื้นคอนกรีตสมรรถนะสูงมากเสริมเส้นใย
เหล็ก

นายคาง เหงวียน ทานห์

วิทยานิพนธ์นี้เป็นส่วนหนึ่งของการศึกษาตามหลักสูตรปริญญาวิศวกรรมศาสตรมหาบัณฑิต
สาขาวิชาวิศวกรรมโยธา ภาควิชาวิศวกรรมโยธา
คณะวิศวกรรมศาสตร์ จุฬาลงกรณ์มหาวิทยาลัย

ปีการศึกษา 2557

ลิขสิทธิ์ของจุฬาลงกรณ์มหาวิทยาลัย

EFFECTS OF CASTING DIRECTION ON PUNCHING SHEAR STRENGTH OF
ULTRA HIGH PERFORMANCE FIBER REINFORCED CONCRETE SLABS

Mr. Tung Nguyen Thanh

A Thesis Submitted in Partial Fulfillment of the Requirements

for the Degree of Master of Engineering Program in Civil Engineering

Department of Civil Engineering

Faculty of Engineering

Chulalongkorn University

Academic Year 2014

Copyright of Chulalongkorn University

Thesis Title	EFFECTS OF CASTING DIRECTION ON PUNCHING SHEAR STRENGTH OF ULTRA HIGH PERFORMANCE FIBER REINFORCED CONCRETE SLABS
By	Mr. Tung Nguyen Thanh
Field of Study	Civil Engineering
Thesis Advisor	Assistant Professor Withit Pansuk, Ph.D.

Accepted by the Faculty of Engineering, Chulalongkorn University in Partial Fulfillment of the Requirements for the Master's Degree

....Dean of the Faculty of Engineering
(Professor Bundhit Eua-arporn, Ph.D.)

THESIS COMMITTEE

....Chairman
(Associate Professor Jaroon Rungamornrat, Ph.D.)
....Thesis Advisor
(Assistant Professor Withit Pansuk, Ph.D.)
....Examiner
(Pitcha Jongvivatsakul, Ph.D.)
....External Examiner
(Professor Piti Sukontasukkul, Ph.D.)

คาง เหงวียน ทานห์ : ผลกระทบของทิศทางการเทต่อกำลังเฉือนทะลุของแผ่นพื้น คอนกรีตสมรรถนะสูงมากเสริมเส้นใยเหล็ก (EFFECTS OF CASTING DIRECTION ON PUNCHING SHEAR STRENGTH OF ULTRA HIGH PERFORMANCE FIBER REINFORCED CONCRETE SLABS) อ.ที่ปรึกษา วิทยานิพนธ์หลัก: ผศ. ดร. วิทิต ปานสุข, 79 หน้า.

แรงเฉือนทะลุซึ่งจัดเป็นพฤติกรรมของโครงสร้างแบบเปราะนั้นได้รับการพิจารณา จัดเป็นรูปแบบการพังทะลายที่พบเห็นได้บ่อยในโครงสร้างพื้น โดยปัจจุบันคอนกรีตสมรรถนะสูง มากเสริมเส้นใยเหล็กซึ่งถือได้ว่าเป็นความสำเร็จครั้งใหม่ของวงการคอนกรีตเทคโนโลยีเนื่องจาก เป็นคอนกรีตที่มีคุณสมบัติเชิงกลที่ดีเยี่ยม นั้นสามารถช่วยในการแก้ปัญหาแรงเฉือนทะลุที่อาจเกิด ขึ้นกับโครงสร้างพื้นบางได้ สำหรับคอนกรีตดังกล่าวคุณสมบัติก่อนและหลังการแตกร้าวจะขึ้นอยู่ กับการเรียงตัวของเส้นใยซึ่งขึ้นอยู่กับวิธีในการเทคอนกรีต ในงานวิจัยนี้ได้ทำการทดสอบตัวอย่าง แผ่นพื้นสี่เหลี่ยมจตุรัสจำนวน 8 แผ่น เพื่อที่จะหาผลกระทบของทิศทางการเทคอนกรีตต่อ ความสามารถในการรับแรงเฉือนทะลุของพื้นและปรับปรุงสมการที่ใช้คำนวณค่ากำลังเฉือนทะลุ ของพื้น ตัวแปรหลักที่ทดสอบได้แก่ปริมาณเส้นใยที่ใช้และทิศทางการเทที่แตกต่างกัน ผลการ ทดสอบที่ได้แสดงว่าการเพิ่มปริมาณเส้นใยนั้นจะเพิ่มน้ำหนักบรรทุกเฉือนทะลุประลัยอย่างมีนัยยะ สำคัญและยังทำให้การปรากฎของรอยแตกร้าวแรกนั้นช้าลงอีกด้วย นอกจากนั้นเส้นใยยังเปลี่ยน รูปแบบการพังทะลายของแผ่นพื้นตัวอย่างจากลักษณะเปราะให้กลายเป็นมีความเหนียวเพิ่มขึ้น โดย พบว่าเมื่อปริมาณเส้นใยเพิ่มขึ้น รอยแตกร้าวจากแรงดัดจะน้อยลงและน้ำหนักบรรทุกเฉือนทะลุ ประลัยจะสูงขึ้น ผลกระทบของทิศทางการเทคอนกรีตสามารถแสดงได้อย่างชัดเจนด้วยขนาดของ การเฉือนทะลุรูปกรวยหงาย แผ่นพื้นที่มีการกระจายตัวของเส้นใยแบบสุ่มจะมีขนาดของการเฉือน ทะลุรูปกรวยหงายเล็กกว่าเมื่อเปรียบเทียบกับแผ่นพื้นที่มีการกระจายตัวของเส้นใยแบบมีทิศทาง สุดท้ายได้มีการเสนอสมการคำนวณค่ากำลังเฉือนทะลุของพื้นคอนกรีตสมรรถนะสูงมากเสริมเส้น ใยเหล็กซึ่งให้ค่าการคำนวณสอดคล้องกับผลการทดสอบเป็นอย่างดี

ภาควิชา	วิศวกรรมโยธา	ลายมือชื่อนิสิต	
สาขาวิชา	วิศวกรรมโยธา	ลายมือชื่อ อ.ที่ปรึกษาหลัก	
ปีการศึกษา	2557		

5670496021 : MAJOR CIVIL ENGINEERING

KEYWORDS: PUNCHING SHEAR / CASTING DIRECTION / THIN SLABS / STEEL FIBERS / FIBERS ORIENTATION / FRC / UHPFRC

TUNG NGUYEN THANH: EFFECTS OF CASTING DIRECTION ON PUNCHING SHEAR STRENGTH OF ULTRA HIGH PERFORMANCE FIBER REINFORCED CONCRETE SLABS. ADVISOR: ASST. PROF. WITHIT PANSUK, Ph.D., 79 pp.

Punching shear, characterized by a brittle behavior, which is considered as the typical failure mode of slab structures. Recently, Ultra High Performance Steel Fiber Reinforced Concrete (UHPFRC) has been known as a new achievement in concrete technology with much superiority mechanical properties which can help people to deal with the problem of punching shear of the thin slab. For UHPFRC material, the properties before and post-cracking mainly depend on the orientation of the fibers, which much depends on the casting method. In this research, an experimental work was conducted on 8 square UHPFRC slabs to investigate the effects of casting direction on punching shear capacity and modify an equation to predict the punching shear strength. The main parameters among these specimens were fibers volume fraction and different casting positions. The results showed that increasing fibers volume can significantly increase the ultimate punching failure load as well as delay the appearance of first cracks. Fibers also change the failure mode of the UHPFRC slabs from brittle to more ductile behavior. The more fibers the less flexural cracks were created and the higher ultimate punching shear failure loads were obtained. The effects of casting direction were clearly illustrated based on the size of failure cone. The slabs with the random distribution of fibers have smaller failure cone while comparing to slabs with the deliberate distribution of fibers. The results from the test and literature review were used to formulate an equation for predicting the punching shear capacity of UHPFRC slabs which gave the good agreement with the experimental results in this study.

Department:	Civil Engineering	Student's Signature	....
Field of Study:	Civil Engineering	Advisor's Signature	....
Academic Year:	2014		

ACKNOWLEDGEMENTS

CONTENTS

LIST OF FIGURES

LIST OF TABLES

CHAPTER 1

INTRODUCTION

1.1 Background of study

For concrete slab structures without shear reinforcement, punching shear regularly is the typical failure mode and it is also considered as one of the most safety aspects required in design of new concrete structures and strengthening the existing concrete structures against punching shear. The punching shear failure is the damage which occurs in a particular zone near the column or loaded area as so-called critical shear perimeter. It might happen when the slabs are subjected to a concentrated force in a small area of concrete section. If the applied load is greater than the resistance capacity of the slabs, then the inclined cracks will appear around the column face or the loading location.

This type of failure is characterized by a brittle behavior. It forms a truncated cone shape at the ultimate failure load and might lead to partially or totally damaged of the whole structures. Despite extensive research about punching shear of the reinforced concrete structure, this problem is still desperately complicated and hard to deeply understand its failure mechanism that the current design approaches often simplify it in practical design.

Since 2000, Ultra High Performance Steel Fibers Reinforced Concrete (UHPFRC) has been recognized as a new achievement in concrete technology. The mechanical properties of UHPFRC is characterized by the high tensile strength with the effects of steel fibers in the mixing, very high compressive strength owing to the very low water/binder ratio, using additive binder, using superplasticizer as water reducing in the mixture components, the strong resistance to corrosion and degradation and excellent performance in term of durability.

The excellent mechanical properties and working behaviors of UHPFRC allow the engineers to design the structure elements to be smaller, thinner and lighter while concrete strength is well-preserved or even better in some individual conditions. Besides many advantages, UHPFRC still has some limitations such as the highly cost in production of this material and the requirement of the cost-effective optimization to guarantee the benefits obtained by applying this kind of concrete in practical design.

As mentioned above, adding steel fibers can enhance the fracture energy, tensile strength and impact resistance. Steel fibers also increase the fatigue resistance of this type of concrete. In addition, it also helps the concrete to reduce the shrinkage and increase the toughness by preventing or delaying the cracks propagation from micro cracks to macro cracks. By using UHPFRC, the engineers can deal with the problem of punching shear of the thin slab which is widely used in building nowadays. The capability of UHPFRC to increase shear and punching shear resistance in structural

elements (e.g. slabs, panels) which is supported by some physical model such as the Modified Compression Field Theory and the Critical Shear Crack Theory.

While studying the mechanical properties and working behaviors of UHPFRC, the researchers found that the strength of the UHPFRC materials before and the mechanisms after cracking much depend on fibers orientation, which considerably depends on the concrete casting procedure. Until now, some researches have studied about this kind of problem but it is still thought-provoking and complex. It is generally due to the lack of standard and procedures in design of UHPFRC structure.

This thesis is an effort to investigate the effects of casting method on fibers orientation and its contribution to punching shear strength of UHPFRC thin slabs. From this experimental work, the test results can apply to modify an equation for checking and calculating the punching shear performance of steel fibers reinforced slab members considering fibers orientation factor in the concrete matrix.

1.2 Objectives of the research

Due to the lack of standards and procedures, it is undeniable that the knowledge and understanding about punching shear mechanism of UHPFRC slabs with some effects of casting direction and orientation of steel fibers still remain margined. Then the main purposes of this thesis herein are listed as shown below:

- To perform the test on UHPFRC slabs about the punching shear failure mode and study the slabs behavior at the failure load.

- To obtain some properties of UHPFRC materials such as compressive capacity, maximum tensile strength obtained from the indirect tensile test method: splitting tensile test and Young's modulus or elastic modulus.

- To investigate the punching shear behavior of UHPFRC slabs without shear strengthening while considering the effects of casting directions and the fibers orientation within the concrete structures.

- To modify an equation for more accurately predicting the punching shear strength of UHPFRC thin slabs taking into account the contribution of steel fibers, concrete tensile strength and steel reinforcement.

1.3 Scopes of the thesis

- The research presented herein basically focused on the investigation of the punching shear behavior of UHPFRC slabs at the ultimate failure load without shear reinforcement. All of the slabs were designed based on the ACI 318-11

2011, American code in metric unit. All of the investigated cases referred to the square slabs.

- The fibers used in this research is the plain steel fiber, straight one typed Dramix OL13/0.20 with some information such as: 13 mm length, 0.20 mm diameter and the aspect ratio is 65. The tension strength is not less than 2000 MPa.

- The flowing method was applied to cast the concrete in this experimental study. The concrete was poured and flowed along an inclined steel plane or chute. The casting positions were chosen at 3 different locations: along one side, at the corner and at the center of the mold. The length of the inclined plane is about 1.60 m and it makes an angle of 20° with the horizontal plane.

- The slab specimens are tested under the punching shear test arrangement particularly designates for this study. In this experiment work, the slabs are considered to fail in punching mode due to the static load only. Another case does not include in this experimental work.

- The main parameters in this study were the fibers volume fraction 0, 0.8 and 1.6 %, three different casting positions as mentioned above. Another parameters such as slab thickness, reinforcement ratio, size factors were not changed in this study.

1.4 Thesis outline

This thesis is organized into five chapters as shown in Figure 1.1. The introduction in Chapter 1 offers the basic knowledge, background, objectives of this study. Scopes and outline of this thesis are provided in this section as well.

Chapter 2 offers the literature review of this study. It is divided into four sections. The first section talked about Fibers Reinforced Concrete (FRC) and Ultra High Performance Steel Fibers Reinforced Concrete (UHPFRC). Their definition, history, mechanism behavior, material properties, advantages and limitations of these types of concrete were reviewed in this section. For the second section, the hypothetical model to calculate the punching shear resistance of FRC and UHPFRC members were detailed. A number of similar works on punching shear of UHPFRC members (slabs) were listed and briefly studied. In the third section, some recommendations which are accepted worldwide in many conferences and symposium about UHPFRC were mentioned. Some internationally recognized standards for investigating the punching shear behavior of reinforced concrete and fibers reinforced concrete slabs were also summarized. And finally, in the fourth section, the orientation effects of steel fibers on the properties of UHPFRC were reviewed.

In Chapter 3, the experimental program in this thesis are introduced. A total of 8 UHPFRC slabs were considered in this thesis which are different in the casting positions and fibers volume fraction. The properties of materials which were used in

this study are given including steel reinforcement, steel fibers, cement, sand and other material. In this study, the effects of casting direction on punching shear capacity of UHPFRC slabs are focused on. So that the concrete casting method and casting procedures are very important in order to obtain the good results. These techniques were described and illustrated by the real photos taken during the time of this study. The properties of UHPFRC such as compressive strength and maximum tensile strength are given. The main specimens design, test setup and the method to collect data are also provided in this part.

1. Introduction

2. Literature Review
- General
- Fiber Reinforced Concrete (FRC)
- Ultra High Performance Fibers Reinforced Concrete (UHPFRC)
- Punching shear of FRC structures
- Fibers orientation in FRC and UHPFRC structures

3. Experimental Program
- General
- Specimens Design
- Materials And Concrete Properties
- Concrete Casting Procedures
- Punching Shear Test Setup

4. Test results and discussions
- General
- Load-deflection curves
- Modes of failure
- Cracks pattern and punching cone size
- Fibers orientations and distributions
- Proposed design equation for punching shear of UHPFRC

5. Conclusions and future prospects

Figure 1.1 Structure of the study

In Chapter 4, all of experimental results and the discussions about the test results are introduced. The load vs. deflection curves of the UHPFRC slabs were mentioned firstly in this chapter. The effects of casting positions and concrete filling method are discussed based on the results from the punching shear test of total 8 slabs. The fibers orientation and distribution in the concrete matrix have the positive influences on punching shear resistance and modify the failure mechanism of UHPFRC from brittle behavior to more ductile behavior. Fibers also help to reduce the size of punching shear cone at the ultimate failure load. However, the combination of steel reinforcement and high percentage of fibers content may have a negative effect due to the fiber blocking if the space between steel reinforcement is not enough and as too much fibers in the concrete matrix. Last but not least, the suggested formula for predicting the failure load, caused by punching shear, of UHPFRC slabs are given. The results from the test and the literature review from the researches of some authors are used to formulate this equation. The proposed design equation is further applied to another researches with the intention of verifying the accuracy.

The conclusions of the experimental work are given with the proposed ideas for the future studies in Chapter 5 of this document.
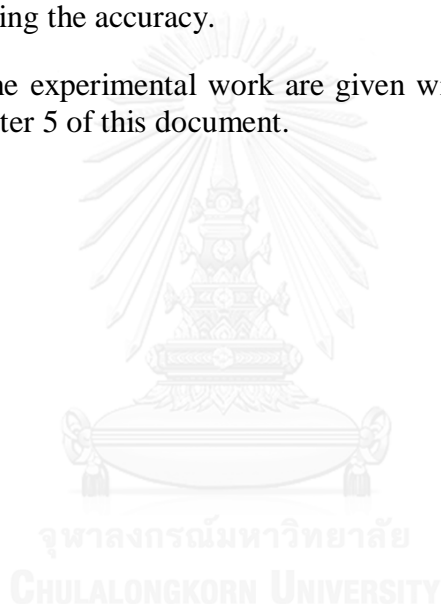
CHAPTER 2
LITERATURE REVIEW

2.1 General

In the last decade, a large number of research has been studied about the punching shear mechanism of reinforced concrete slabs and fibers reinforced concrete slabs. Many experimental studies have accomplished and the researchers have proposed some theoretical and analytical models to investigate the punching shear resistance of reinforced concrete and fibers reinforced concrete slabs. In this chapter, in order to get the basic knowledge and the idea for supporting this thesis, many experimental works, theories and researches were listed and reviewed. Considering the extensive researches on punching of slabs, a completed review of all experimental investigations and developed models would go beyond the scopes of this study.

Chapter 2 gives the brief overview of the developments of some studies about the punching shear strength of fiber reinforced concrete members with and without the shear strengthening, then the literature review is divided into four sections.

- The first section talked about Fibers Reinforced Concrete (FRC) and Ultra High Performance Steel Fibers Reinforced Concrete (UHPFRC). The definition, history, mechanism behaviors, material properties, advantages and disadvantages or limitations of these types of concrete would be reviewed in this section.

- The second section, the hypothetical model for calculating the punching shear performance of FRC and UHPFRC members were detailed. A number of similar works on punching shear of UHPFRC members (slabs) were listed and also briefly reviewed.

- In the third section, some recommendations which was accepted worldwide in many conferences and symposium about UHPFRC were mentioned. Some internationally recognized standards for punching shear resistance of reinforced concrete slab and fibers reinforced concrete slabs would be summarized such as American code (ACI 318-11) [1], European code (EC2-2004) [2], Japanese Standard for Concrete Structures (JSCE) [3] and French Association of Civil Engineers (AFGC) [4].

- Finally, in section four, some orientation effects of steel fibers on the properties of UHPFRC were reviewed. The main factors contributed to the distribution and orientation of steel fibers would be overviewed such as concrete casting direction, casting procedure, size and shape effects. Some current methods to determine the fibers distribution and fibers orientation were reviewed; following by some related works would be listed and outlined.

2.2 Fibers reinforced concrete (FRC)

FRC is one important invention in field of construction materials and it was considered as the turning point opening a revolution in concrete technology. FRC is widely used in construction works nowadays. By using this kind of concrete, the structural engineers can design and build concrete elements from normal strength concrete to high strength concrete, the structures have strong resistance against tensile forces as well as the convenience in construction and the minimization of maintenance cost.

FRC was applied in many types of structures in many fields of civil engineering such as long span bridges, high-rise buildings, highway overlays, runway at the airport and others special concrete structures (e.g. tunnel, marine structures, wind power foundation). In the years of 1950s, Portland Cement Association began to study fibers as reinforced elements and developed its applications in construction, which was considered as the milestones, opened a new period for the development of FRC. However, the development of FRC was not really considered until 1960's. There was a great expansion in the research topic of fiber reinforced concrete structures, especially in FRC applications. Many researchers were performed the experimental study about FRC following with the development of structural applications and the optimization of the mixing proportions of this new material.

| a) | b) | c) | d) |
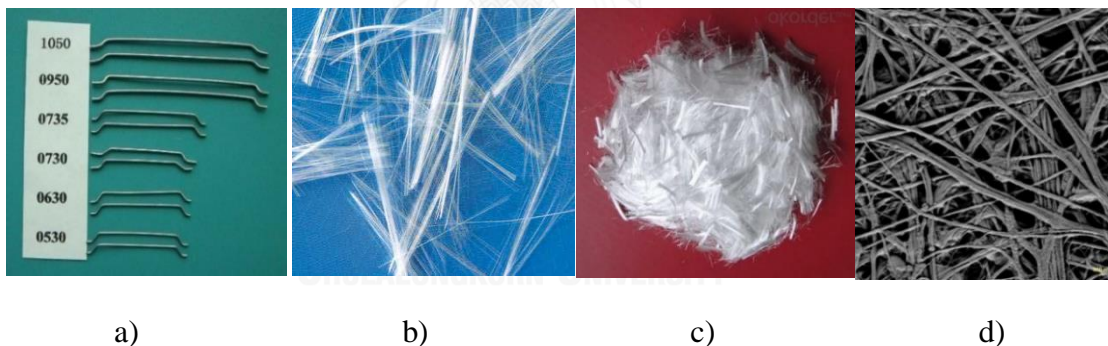
Figure 2.1 Typical types of fibers on the market [5]

The more applications were identified, more types of fibers were introduced to the world market. Figure 2.1 had introduced some kinds of fibers which were commonly used in the research and the actual construction work such as steel fibers (Figure 2.1a), glass fibers (Figure 2.1b), polypropylene fibers (Figure 2.1c), carbon fibers and natural organic fibers (Figure 2.1d).

Among these types of fibers, steel fibers were the most important and most popular used in construction works thanks to the excellence properties obtained when mixing it with reinforced concrete to create a high performance cementitious composites matrix. Understanding that the collaboration of the fibers and the concrete which would determine the concrete quality, many experiments about FRC had been performed in the years recently. The results had come together with the appearance of new types of fibers reinforced concrete as presented in Figure 2.2.
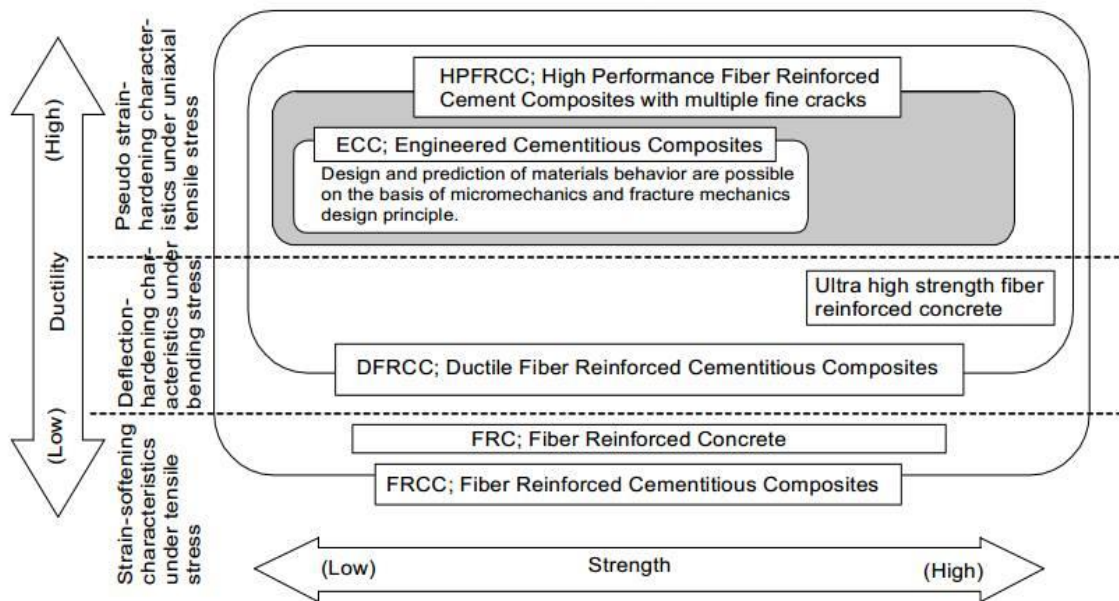
Figure 2.2 Classification of fiber reinforced concrete [3]

In Figure 2.2, Fibers Reinforced Cementitious Composites (FRCC) is the general name of many types of FRC. According to Japanese Society of Civil Engineering, FRCC are classified into some groups with the difference in the concrete strength and ductility of fresh concrete such as ECC, RPC, HPFRCC and UHPFRC. Engineered Cementitious Composite (ECC) was a kind of FRC with the fibers volumes up to 20 %. This materials showed a higher toughness than conventional FRC. In 1990s, Pierre Richard had developed Reactive Powder Concrete (RPC), an extraordinary strength, great ductility cementitious composite and many excellent physical properties and working behavior.

The development of RPC led to the introduction of UHPFRC characterized by the very high compressive strength between 150 MPa and 250 MPa, high ductility, elastic limit in tension reached to 10 MPa. In 1997, the Sherbrook Bridge in Quebec, Canada, the first Ductal® ultra-high performance concrete bridge in the world, was constructed. Since the 2000s, UHPFRC has been achieved much significant rewards with a large number of applications and became a prospective material in the construction and also in material science field.

2.3 Ultra high performance fibers reinforced concrete (UHPFRC)

Ultra High Performance Steel Fibers Reinforced Concrete (UHPFRC) has been known as a potential material that can adapt many requirements in construction field nowadays. Thanks to the excellent characteristic under compressive and tensile loading, the very high strength and strain hardening performance after cracking, the UHPFRC structural elements can resist to severe forces and environmental actions such as blast load,

freezing and thawing actions. Coarse aggregates were removed from the mixing components and fine aggregates were used instead of normal aggregates in the mixture of UHPFRC. This reason can explain why UHPFRC has a homogenous and compacted cementitious matrix that offers very high strength and strong toughness to the structural members (compressive strength is over 150 MPa, maximum tensile strength can be more than 10 MPa).

In UHPFRC, the water/binder ratio is very low, usually is not over than 0.2 and the fibers volume ratio is varied from 1 to 2 % for the typical UHPFRC mix. By adding the steel fibers into the mix, the cement matrix shows a higher bond capacity and increases the ductility of the mixture. Moreover, the bridging effects between steel fibers offers a strain hardening response with high tensile strength before and after cracking. The appearance of steel fibers inside the mix also adjusts the brittle failure mode in compression to a more ductile failure mode, increases the micro strengthening and avoids the unpredicted explosive failure in compression.

2.3.1 Mix design of UHPFRC

The mix design of UHPFRC is distinct from that of conventional concrete and concrete with high strength. It is characterized by the high content of cement, super plasticizer and silica fume. Especially, the water/binder ratio regularly is very low, less than 0.20. The mixtures of UHPFRC include: Portland cement, silica fume powder, fine sand, fibers, water and water reducing product or super plasticizer. The ratio between water and binder often varies from 0.14 to 0.20 with high percentage of silica fume up to 20 % of cement weight. The steel fibers for UHPFRC is up to 2 % of batch volume and superplasticizer is up to 2 % of cement weight.

Due to the high cost in the production of UHPFRC that the optimization of the mix design is one of requirement to ensure the economic benefit. To do that, many research were concerned about this problem in order to find a best mix proportions (the cheaper mix design but still adaptable with the target design strength requirement). According to Tuan [6], he tried to add some waste materials into the mix of UHPC or UHPFRC to reduce the cost. He found that some local materials can be used to replace the more expensive ones in the UHPFRC mix components. He studied the probability of using rice husk ash (RHA), a very popular substance in Vietnam, to substitute some amount of silica fume in the UHPC components. From the experimental results, this author stated that the value of compressive stress of UHPC can reach 150 MPa in some cases.

Another researcher was Yang [7]. In his study, he used the recycling material from crystal cullet besides two kinds of sand in local area to substitute silica sand, an expensive material, which is used in UHPFRC. Nevertheless, the experimental results showed that the performance of this specimen was lower 15% approximately than the normal UHPFRC specimens (i.e. compressive strength, flexural capacity and fracture energy).

In the research of Yu [8], he also studied about the mix design and evaluated the properties of UHPFRC. The aim of his research was able to obtain a high density cementitious matrix with a low binder amount and also a low porosity. The workability, air content, permeability, flexural and compressive strengths were investigated and analyzed. The experiment results specified that it was capable to design this material with a low binder quantity. He also calculated the cement hydration degree. He found that, after 28 days of curing, there was still a large amount of unhydrated cement in the concrete matrix. So it could be substituted by grouts to increase the workability and productivity.

2.3.2 Compressive strength UHPFRC

UHPFRC is categorized as a high compressive strength materials (or even very high) with the compressive strength is usually more than 150 MPa at 28 days after curing in normal condition and can reach 250 MPa in some special curing conditions. The high compressive strength can be explained by eliminating coarse aggregates and using only fine grain sand that can create a homogeneous and compact matrix. When UHPFRC was subjected to compression loading, it showed a ductile behavior after reaching to the peak load. The modulus of elasticity at 28 days is also high and varies from 50 to 70 GPa. UHPC normally shows brittle performance under compression, while the introduction of steel fibers into the mix design of UHPFRC reduces the influence of the brittle behavior and also improves the compressive strength compared with that of the conventional concrete and UHPC as demonstrated in Figure 2.3.
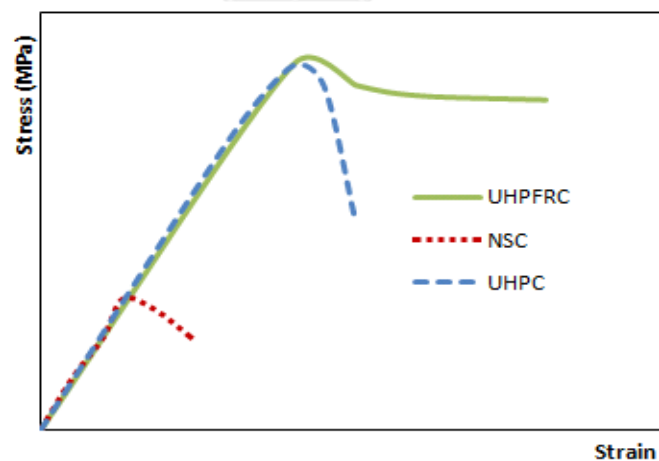
Figure 2.3 Stress-strain curve of UHPFRC, NSC and UHPC in compression [9]

Figure 2.3 showed the comparison of the compressive strength behavior between UHPFRC, UHPC without fibers and normal strength concrete (NSC). The UHPFRC behavior in compression was almost straight before it reached the peak load and it was quite similar to the UHPC behavior. But after peak load, UHPFRC behavior was nonlinear while UHPC showed a very brittle behavior, the curve went down vastly after reaching the peak load. It can be explained by the bridging effects of fibers and stress transfer mechanism of the micro cracks.

2.3.3 Tensile strength UHPFRC

Tensile strength is the most different characteristic between UHPFRC and conventional FRC. It mostly mentions to two aspects such as the first cracking point and the post cracking mechanism and behavior. Fibers can help the matrix to resist higher forces and finally strengthen the structures. The comparison between the typical stress-strain curve of UHPFRC and conventional FRC was shown in Figure 2.4.

Figure 2.4 Typical stress-strain curve of UHPFRC and FRC in tension [10]

These stress-strain curves are divided by 3 parts to make the comparison between two types of concrete:

- Part I: The curves is straight (linear) until A in both Conventional FRC and UHPFRC, the stress increase is quasi linear elastic until the stress reaches the cracking stress σ_{cc} .

- Part II: It is followed by multiple cracking curve until B with a post cracking stress σ_{pc} for UHPFRC while the post cracking stress decreases within this part of FRC. It is called strain hardening curve for UHPFRC because the post cracking capacity is higher than the cracking stress.

- Part III: The first crack starts at B. After that, the crack is propagating and the crack width is increasing until the failure happened. This curve is called softening branch.

To obtain the post cracking behavior of UHPFRC, the uniaxial tensile test is considered as the best method in the theoretical point of view. But it is time intensive, therefore, standard method usually is the bending tests on prisms or plates.

2.4 Punching shear

2.4.1 Problem statement

Punching shear failure is often considered as the critical failure mode for the design of reinforced concrete floors and slabs. When a slab is subjected to a concentrated load over than the capacity, the failure is called as punching shear or two way shear. Figure 2.5 showed two examples of total collapse of the structure due to the punching shear failure at the car park in Christchurch, New Zealand (Figure 2.5a) and Wolver Hampton, United Kingdom (Figure 2.5b).

a)   b)
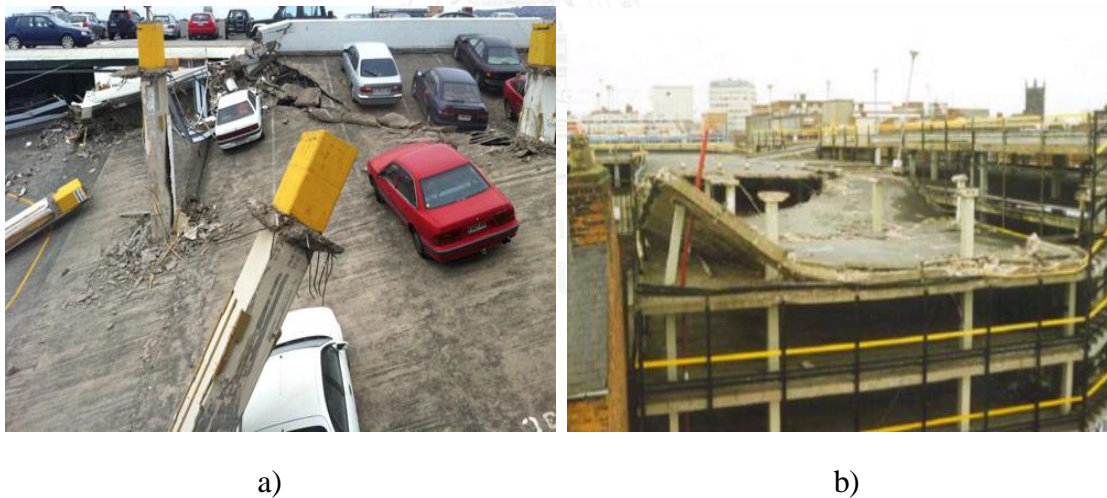
Figure 2.5 Examples of structures failed in punching shear mode a) Christchurch, New Zealand; b) Wolver Hampton, United Kingdom [11]

This type of failure is a fragile failure behavior and may cause the local failure or even total damage of the structure. It takes place around the loaded region, formulates a truncated cone shape separated with the others part of the slab by the diagonal tensile cracks. In despite of many researches in this subject, punching shear failure still remains as a complicated problem that the current design code is often simplified or even empirical this phenomenon.

2.4.2 Punching shear theory

2.4.2.1 Kinnunen and Nylander Model [12]

Based on the tests of 61 circular slabs, Kinnunen & Nylander offered the first concept to compute the punching shear performance of reinforced concrete slab elements lacking of transversal reinforcement in 1960 [12]. The specimens were held by a short column at center of each slab and loaded on the borderline as shown in Figure 2.6. The creation of shear and punching shear crack, the deformation shape and the strain of reinforcement were there main factors of this research. The ultimate failure shape formed a truncated cone limited by the shear cracks and rigid elements separated by the radial cracks.
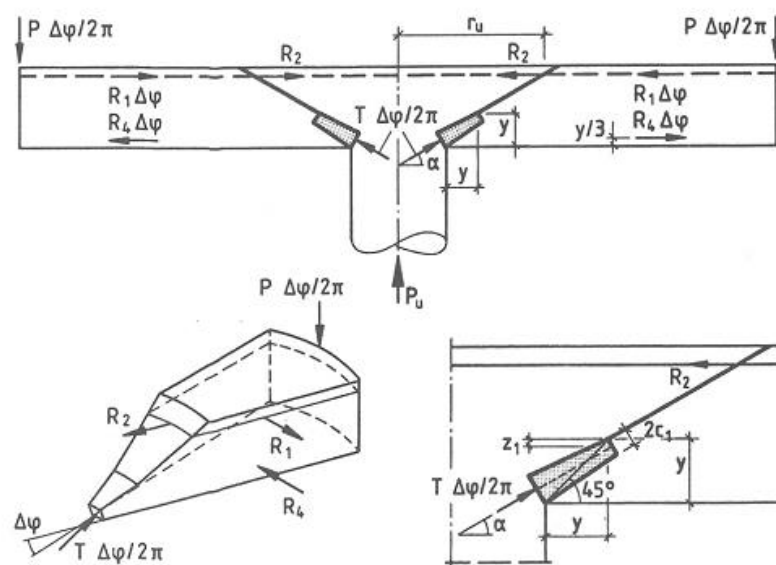
Figure 2.6 Proposed model for punching shear by Kinnunen & Nylander [12]

The main idea of this study was the formation of an equilibrium forces system acting on the separated rigid elements. While observing the testing procedure, Kinnunen & Nylander had detected that the slab segment behavior was close to a rigid body action. When the load increases, the segment rotates with an angle ψ. The segment internal forces were balanced with the applying forces on the perimeter. The stress were the functions of the slab's rotation and the mechanical behavior of and steel reinforcement concrete. The conditional failure was assumed to take place when the compressive stress in the strut and tangential strains at the points located under the central of the rotation reached their critical values. The ultimate load was determined by using the equilibrium equations and the failure criteria.

The ultimate predicted load P_u was obtained by three equilibrium equations: one equilibrium equation of the vertical forces and two equilibrium of the flexural moments. The model of Kinnunen and Nylander showed that punching shear capability of reinforced concrete slab is governed by some factors such as compressive strength of concrete, column size, slab thickness and steel reinforcement ratio. This model was further developed by Kinnunen for orthogonal, two ways reinforcement slabs (1962) and Anderson for slabs with shear reinforcement (1963).

2.4.2.2 Critical Shear Crack Theory

Based on the Kinnunen & Nylander model, Muttoni & Schwartz had further developed the punching shear model by considering the appearance of critical shear crack [13], [14], [15]. They observed that the punching stress decreases when the slab rotation increases.
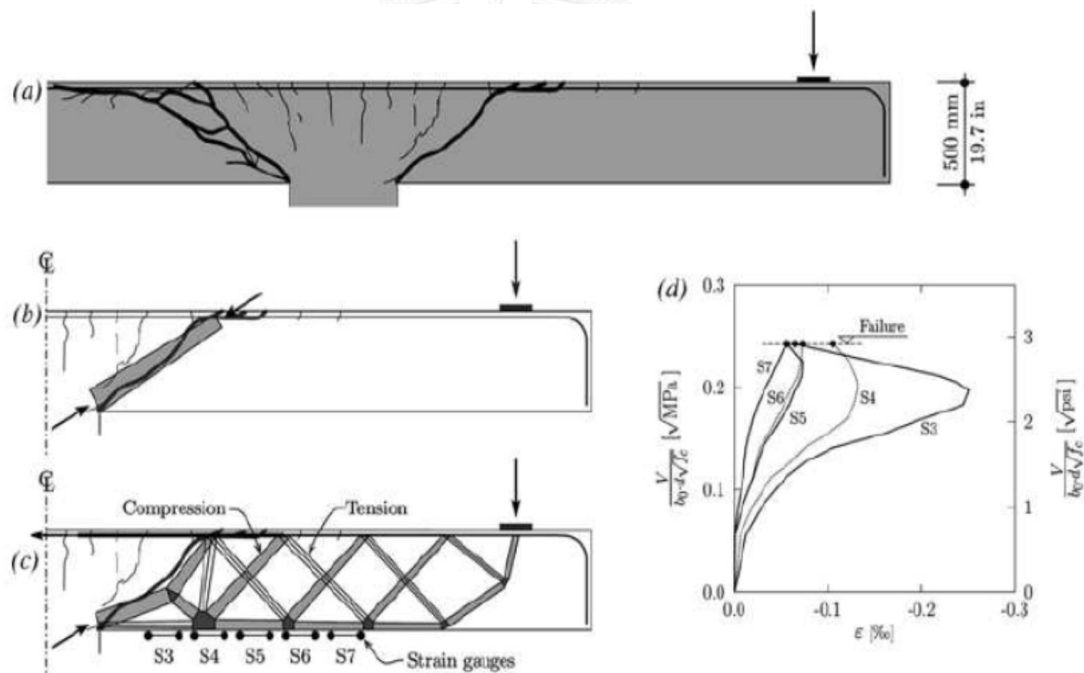
Figure 2.7 Punching test by Guandalini and Muttoni [15]

This phenomenon could be explained because the existence of critical crack caused by shear that reduces strength capacity of the inclined compressive strut which carries the shear stress and may lead to the failures of the specimens as can be illustrated in Figure 2.7a and 2.7b. After reaching a maximum values, the radial compressive strain decreases and the tensile strain may be obtained. These strains may be described by the appearance of the nudge strut and a tensile component along the top face as a result of the critical shear crack expansion as shown in Figure 2.7c.

Based on this observation, Muttoni & Guandalini [16] had proposed a model for punching shear failure. In this theory, they supposed that the opening of the grave shear cracking had a relation with the rotation ψ of the slab and the average effective depth d of the specimens. They proposed an equation for calculating the punching shear failure as shown in equation (1) below:

$$\frac{V_{pc,c}}{ud\sqrt[3]{f_c}} = \frac{1}{1+\dfrac{\psi d}{4}} \tag{1}$$

Muttoni and his teams had further developed their equation for the punching shear in 2003. Based on the research of Walraven & Vecchio about the aggregates interlock, he found that the roughness of the crack affected the shear transferred across the critical shear crack and this shear stress can be carried by the aggregates interlock by means of dividing the nominal crack width by the aggregate sizes as shown in equation (2) as follows:

$$\tau_R = \frac{V_R}{ud} = \frac{0.3\cdot\sqrt{f_c}}{0.4+0.125\psi d\left(\dfrac{48}{d_{g0}+d_g}\right)} \tag{2}$$

where τ_R: nominal shear strength, u: critical perimeter, d_g and d_{g0}: the largest size of coarse aggregate and the reference size taken as 16 mm, respectively, f_c: compressive strength of the cylindrical specimens.

2.4.3 Existing equations for punching shear

2.4.3.1 Narayanan and Darwish [17]

With the intention of improving the punching shear capacity of micro-concrete slabs, Narayanan and Darwish had studied the effects of using short steel fibers as the reinforcement by conducting the experiment works on 12 slabs which are simply supported [17].

The main factors in this work were the content of fibers in volume, the tensile reinforcement ratio, and the strength of concrete. The data showed that by increasing fibers volume percentage the shear strength increased as well and adjusted the location of the critical shear crack. These authors suggested that the practical design of punching shear can be the same way which was applied for beams and proposed an equation for computing the punching shear strength of slabs as the following:

$$v_{pc} = \xi_s \left(0.24 f_{sp} + 16\rho + v_b \right) \tag{3}$$

where ξ_s: empirical depth factor, f_{sp}: splitting tensile stress of fibers reinforced concrete, ρ: ratio of tensile reinforcement, v_b: vertical pull-out stress of fibers along the inclined cracks.

Based on this model, Tan and Paramasivam [18] had modified equation (3) to propose their formula for measuring the punching shear resistance of slabs as given in equation (4) below:

$$V_{pc} = \xi_s (0.24 f_{sp} + 16\rho + 0.41\tau_b v_f a_f \frac{l_f}{d_f}) u_b d \tag{4}$$

$$u_b = (1 - 0.55 v_f a_f \frac{l_f}{d_f})(4e + 3\pi h) \tag{5}$$

where u_b: critical perimeter, h: slab thickness, e: width of loading plate, d and ξ_s: effective depth and empirical depth factor, $\xi_s = 1.6 - 0.002h$, τ_b: the average fibers matrix interfacial bond stress ($\tau_b = 4.15$ MPa),

v_f: content of steel fibers in percent of volume, a_f factor for fibers type (can be taken as 0.5, 0.75 and 1 for round, crimped and duo form fiber), l_f and d_f are the length and the diameter of fibers, respectively.

2.4.3.2 Harajli et al. [19]

Harajli [19] and his team had considered the steel fibers influences on punching shear behavior of flat slabs by testing 12 series of small size FRC slab-column connection. The varying parameters involved the type of fibers, the amount and aspect ratio of fibers, and the proportion of the span over the depth of these specimens. From the test results, it indicated that the shear failure ductility can significantly improve by adding the hooked-end steel fibers to the concrete mixture, adjust the failure behavior from pure punching to flexural, and their ultimate shear capacity significant increases as the results. The final shear strength was nearly dependent on the fibers content.

According to the experimental results and others experimental data, these authors had proposed an equation to measure the maximum resistance against punching shear failure of slab-column connections considering the steel fibers reinforcement as follows:

$$V_{pc} = \left(0.033 + 0.075 v_f\right) \cdot b_0 d \sqrt{f_c} \tag{6}$$

where v_f : content of steel fibers, b_0 : critical shear failure perimeter, d : effective depth and f_c is the compressive strength of concrete cylindrical specimens.

2.4.3.3 Muttoni and Ruiz [14]

Muttoni and Ruiz [14] had proposed the formula for predicting the resistance of FRC slabs against punching shear failure which is supported by the Critical Shear Crack Theory. The slabs did not contain any transverse reinforcement. The calculation had been taken by considering the contribution of concrete $V_{pc,c}$ combining with the governing part of steel fiber $V_{pc,f}$ to the ultimate punching shear strength as shown in equation (7) below:

$$V_{pc} = V_{pc,c} + V_{pc,f} \tag{7}$$

$V_{pc,c}$ and $V_{pc,f}$ are defined as equation (8) and (9) below:

$$\frac{V_{pc,c}}{ud\sqrt{f_c}} = \frac{3/4}{1 + 15\left(\dfrac{\psi d}{d_{g0} + d_g}\right)} \tag{8}$$

where u : critical perimeter taken at distance $d/2$ started at the column face, d is the effective depth, f_c is the concrete compressive strength, ψ is the specimens slab rotation.

$$V_{pc,f} = \sigma_{tf}(w) A_p = \sigma_{tf}\left(\frac{\psi d}{6}\right) A_p \tag{9}$$

$$\sigma_{tf} = k_f \alpha_f \rho_f \tau_b \tag{10}$$

$$k_f = \frac{1}{\pi} \arctan\left(\alpha_e \frac{w}{d_f}\right)\left(1 - \frac{2w}{l_f}\right)^2 \tag{11}$$

$$\tau_b = k_b \sqrt{f_c} \tag{12}$$

where σ_{tf} : bridging stress of steel fibers, w : the critical shear crack opening, A_p : the area of punching shear failure surface projected on horizontally plane, k_f : global

orientation factor, α_f : aspect ratio of fibers, ρ_f : fibers volume ratio, τ_b : bonding stress between fibers and concrete, α_e : fibers engagement factor (taken as 3.5 for normal condition),

k_b is the bonding factor (set as 0.8 for hooked ends fibers, 0.6 for crimped fibers, 0.4 for straight fibers).

2.4.3.4 Higashiyama et al. [20]

In this study, the proposed formula was based on the JSCE equation. Higashiyama [20] had considered the effect of the fibers pull-out force presented by Narayanan and Kareem-Palanjian [21] and the dimension of the critical section presented by Narayanan and Darwish [17]. The prediction equation is calculated by the following equations:

$$V_{pc} = \beta_d \beta_p \beta_r (f_{pcd} + v_b) u_p d \tag{13}$$

$$f_{pcd} = 0.2\sqrt{f_c} \; < 1.2 \text{ MPa} \tag{14}$$

$$\beta_d = \sqrt[4]{1000/d} \; <1.5 \tag{15}$$

$$\beta_p = \sqrt[3]{100\rho} \; <1.5 \tag{16}$$

$$\beta_r = 1 + \frac{1}{1 + 0.25u/d} \tag{17}$$

$$v_b = 0.41\tau_b F \tag{18}$$

$$u_p = (u + \pi d)(1 - KF) \tag{19}$$

$$F = \frac{l_f}{d_f} V_f a_f \tag{20}$$

where τ_b : average fibers-concrete bonding stress (τ_b =4.15 MPa), f_c is the cylindrical compressive strength,

u_p : perimeter of the critical section at distance $d/2$ from the loaded area, u : perimeter of the loaded area,

K : non-dimensional constant value (K =0.32), F is the fibers factor.

2.4.4 Current standard for punching shear of RC slabs

2.4.4.1 ACI 318-11 [1]

    a) Slabs without shear reinforcement

ACI 318-11 proposes that the punching shear capacity of nonprestressed slab without shear strengthening is the minimum value which is calculated by three equations (21), (22), (23) as follows:

$$V_{pc} = 0.083\left(2 + \frac{\alpha_s d}{b_0}\right)\lambda\sqrt{f_c'}b_0 d \tag{21}$$

$$V_{pc} = 0.17\left(1 + \frac{2}{\beta}\right)\lambda\sqrt{f_c'}b_0 d \tag{22}$$

$$V_{pc} = 0.33\lambda\sqrt{f_c'}b_0 d \tag{23}$$

where λ: concrete density factor (taken as 1.0 for normal concrete and 0.8 for low density concrete), β: column size factor defined by the ratio between the long side and short side of the column, b_0: control perimeter,

f_c': compressive strength of concrete in MPa, α_s: coefficient (set as 40, 30 and 20 for interior columns, edge columns and corner columns, respectively).

In case of prestressed slabs, the ultimate punching shear force can be calculated by equation (24) as follows:

$$V_{pc} = (\beta_p\lambda\sqrt{f_c'} + 0.3f_{pc})b_0 d + V_p \tag{24}$$

where β_p: smaller value between 0.29 and $0.083(\alpha_s d / b_0 + 1.5)$,b_0 : the control perimeter, f_{pc} : the average intensity of effective prestress on control perimeter, V_p : the vertical part of all effective prestress forces crossing the critical section.

    b) Slabs with shear reinforcement

According to ACI 318-11, failure caused by punching shear within the area which is shear-reinforced can be considered by adding the contribution of shear strengthening to the concrete contribution. Thus, the final formula for calculating the punching shear resistance of the slabs with stirrups is defined as:

$$V_{pc} = 0.17\lambda\sqrt{f_c'}b_0 d + \frac{A_v f_{yt} d}{s} \tag{25}$$

where b_0: control perimeter taken from the distance of $d/2$ from the border of the support surface, d and f_c': effective depth and compressive capability of concrete, respectively,

s: the distance between perimeters of shear reinforcement, A_v: cross-sectional area of one perimeter of shear reinforcement within spacing s, and f_{yt}: the yield strength of the shear reinforcement.

2.4.4.2 Euro Code 2 [2]

a) Slabs without shear reinforcement

While comparing to ACI 318-11, the provision of EC2 2004 had some differences in taking account of the flexural reinforcement ratio and size effects. Figure 2.8 showed the suitable authentication model for inspecting the punching shear failure at the final stage based on Euro code EC2.

Thus, the punching strength for slabs lacking of shear reinforcement is defined as:

$$V_{pc} = \frac{0.18}{\gamma_c}k(100\rho_l f_c)^{1/3} + 0.1\sigma_{cp} \geq (v_{min} + 0.1\sigma_{cp}) \tag{26}$$

$$k = 1 + \sqrt{\frac{200}{d}} \leq 2.0 \tag{27}$$

$$\rho_l = \sqrt{\rho_{ly}\cdot\rho_{lz}} \leq 0.02 \tag{28}$$

$$\sigma_{cp} = \frac{\sigma_{cy} + \sigma_{cz}}{2} \tag{29}$$

$$\sigma_{cy} = \frac{N_{Ed,y}}{A_{cy}} \tag{30}$$

$$\sigma_{cz} = \frac{N_{Ed,z}}{A_{cz}} \tag{31}$$

where f_c : compressive stress of concrete, d : effective depth of the slab, ρ_{ly}, ρ_{lz} related to the bonding of tensile steel in y and z axis, σ_{cy}, σ_{cz} : normal stresses of concrete in the critical part in y and z axis,

$N_{ed,y}, N_{ed,z}$: longitudinal forces across the full bay for internal column and the longitudinal forces across the control section for edge column, A_c is the area of concrete according to the definition of N_{ed} , v_{min} is the minimum punching shear stress ($v_{min} = 0.035k^{3/2}f_c^{1/2}$).
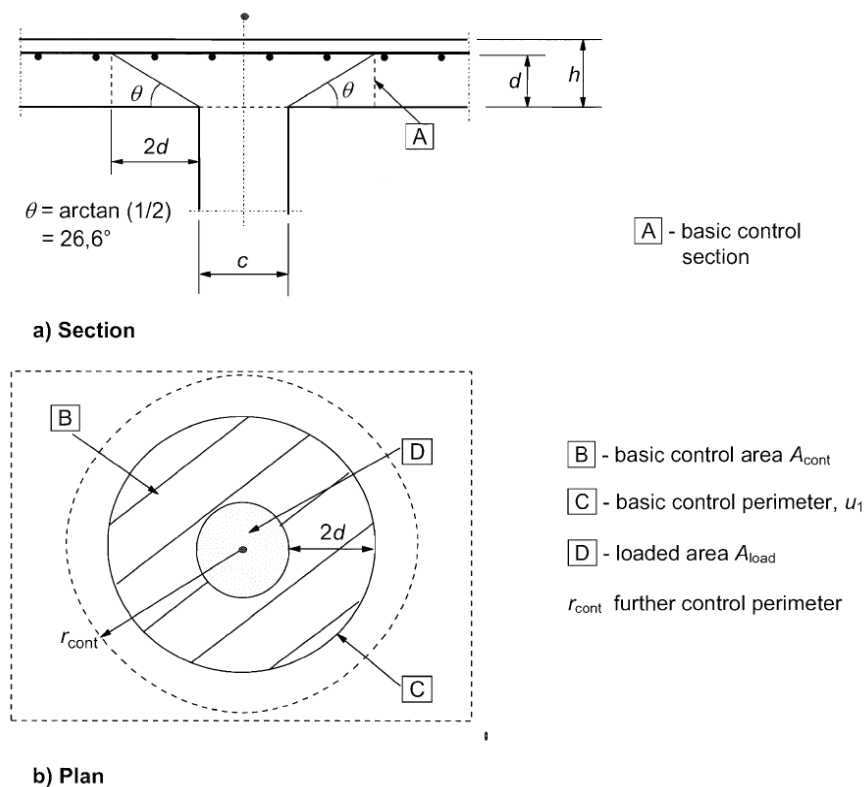
Figure 2.8 Control section for punching shear according to EC2 [2]

b) Slabs with shear reinforcement

Similar to ACI 318-11, Euro Code proposes the combination of the concrete contribution together with the shear reinforcement contribution, whereby the concrete contribution corresponds to 75% of the punching strength of slabs with no shear strengthening. Thus, the punching strength could be calculated as:

$$V_{pc} = 0.75V_{pc,c} + 1.5(d/s_r)A_{sw}f_{ywd,ef}(1/(u_1 d))\sin \alpha \qquad (32)$$

$$f_{ywd,ef} = 250 + 0.25d \le f_{ywd} \qquad (33)$$

where A_{sw} : area of one perimeter of shear strengthening nearby the column, s_w : radial spacing of perimeters of shear reinforcement,

d : mean of effective depth, $f_{ywd,ef}$: effective design strength of the shear reinforcement, α : angle between the shear strengthening and the plane of the slab.

2.4.4.3 JSCE Recommendations [3]

The Japan Society of Civil Engineers (JSCE) have offered the "Recommendations for Design and Construction of High Performance Fibers Reinforced Cement Composites with Multiple Fine Crack" (HPFRCC) in which, they presented an equation to calculate the punching shear capability of planar concrete structures made by HPFRCC subjected to concentrated loading as follows:

$$V_{pc} = V_{pcd} + V_{pcf} \tag{34}$$

where V_{pcd} is the design punching shear strength by considering the fibers contribution only, specified by equation (35) and V_{pcf} is the design punching shear capability exerted by strengthening fibers, specified by equation (40):

$$V_{pcd} = \beta_d \beta_p \beta_r f'_{pcd} u_p d / \gamma_b \tag{35}$$

$$f'_{pcd} = 0.7 \cdot 0.20 \cdot \sqrt[3]{f'_{cd}} \ \ (\text{N/mm}^2), \text{ where } f'_{pcd} \leq 0.84 \ \ (\text{N/mm}^2) \tag{36}$$

$$\beta_d = \sqrt[4]{1000/d} \ , \ \beta_d \text{ is not more than 1.5} \tag{37}$$

$$\beta_p = \sqrt[3]{100\rho} \ , \ \beta_p \text{ is not more than 1.5} \tag{38}$$

$$\beta_r = 1 + \frac{1}{1 + 0.25u/d} \tag{39}$$

$$V_{pcf} = f_{vd} u_p d / \gamma_b \tag{40}$$

where f'_{cd} : target compressive strength (N/mm^2), u : perimeter of loaded section, u_p : exterior perimeter of the design cross section at the distance $d/2$ from the loading section, d : effective depth, p : tensile reinforcing ratio, γ_b : element parameter (taken as 1.3 in general case), f_{vd} : design tensile yield strength of HPFRCC in the direction orthogonal to the diagonal crack direction, $f_{vd} = 0$ once f_{vd} is less than 1.5 N/mm^2.

2.4.4.4 AFGC recommendations on UHPFRC [4]

This document was published in 2013. It is a new version of "French Association for Civil Engineers" (AFGC) recommendations on UHPFRC first published in January 2002. The new version was drafted by the AFGC/SETRA working group on Ultra High Performance Steel Fibers Reinforced Concrete chaired by Jacques Resplendino.

The new version, mainly motivated by the compatibility with entering in force of the Euro codes. The AFGC equation for calculating the punching shear resistance of UHPFRC elements is given in the following equation;

Considering a reference contour positioned at a distance of $h/2$ from the loading position, the shearing stress τ must be less than:

$$\tau_{max} = 0.8 \frac{f_{ct}}{K_{local} \cdot \gamma_{cf}} \tag{41}$$

where $f_{ct} = \min\left(f_{ctfk}, f_{ctk,el}\right)$ in the case of thick elements, f_{ctfk} is the tensile stress derived from the tensile tests, $f_{ctk,el}$ is the characteristic elastic tensile strength, K_{local} is the fibers orientation coefficient for local effects (K_{local} is taken as 1.75), γ_{cf} is the partial safety factor (set as 1.3 in the case of durable/transient and 1.05 in the case of accidental situations).

2.5 Fibers orientation

2.5.1 Problem statement

FRC and UHPFRC are two types of concrete which were regarded as the important inventions, opened the new period in construction materials field. Fibers have been introduced to the mix with the purpose of improving the mechanical properties in the hardening phase of the concrete matrix such as increasing the concrete tensile strength, shear strength, decreasing the shrinkage and developing its capacity to resist the abrasion, fatigue, fire resistance and impact behavior. In FRC and UHPFRC structures, the distribution and orientation of fibers have been known as one of the most factors had a large effect on the material properties according to the researches of Grunewald [22], Pansuk [23] and Kim [24]. In production procedure, the distribution and orientation of fibers may be affected by many factors such as the fibers volume ratio, the early aged properties of concrete, the flow ability of the mix, the casting method, the concrete casting position, the size and dimension of the formwork and the vibration method. In the next following paragraphs, some factors will be listed and detailed.

2.5.2 Factors influencing fibers orientation

As mentioned above, the dispersal and orientation of steel fibers over the concrete surface and within concrete matrix might be exaggerated by the amount of fibers and dimension of the specimens, along with the flow ability of the concrete mixture and the compaction manner. The experimental study on the early phase working behaviors of FRC performed by some authors including Grunewald [22], Kooiman [25] Martinie and Roussel [26] stated that the orientation and distribution of fibers, which effected the hardened characteristic of concrete, are influenced by the flow of fresh concrete. Martinie et al. had proposed two reasons which most affected the orientation of fibers namely as the "wall-effect" that depended on the size, shape and dimension of the mold and the fresh early aged flow ability of the concrete mix, which was governed by the material behaviors, the geometry of the mold and the concrete casting method.

The factor most affecting the fibers orientation is the concrete flow. Martinie and Roussel had performed the test on many specimens to investigate how much the concrete flow contributed to the fibers orientation [26]. They used two types of channel flow (freely flow on the surface and restrained flow) to make the difference in the flow of concrete. The experimental results stated that fibers have a trend to align along the concrete flow direction in the confined channel flow condition.

Another researches had given the evidence that the casting procedure may influence the fibers orientation [27], [28]. Barnett et al. tried the test on several round plates of UHPFRC by casting concrete at different positions (from the middle, from the side, and randomly). The results from X-Ray CT image scanning showed that these casting positions caused the difference of fibers orientation in the samples, thus, the load resistance and flexural strength of these samples were considerably changed (up to 67 % and 120 % respectively). Furthermore, the length of fibers might also take into account to the orientation of fibers.
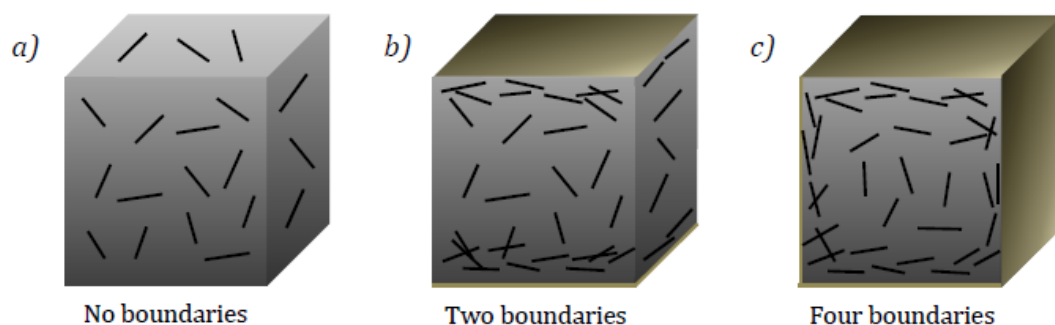
Figure 2.9 The effects of boundary restraints to the fibers orientation [29]

With the intention of describing the effects of geometry and boundary conditions on fibers orientation, many researchers used the name "wall-effect" to demonstrate this phenomenon as shown in Figure 2.9. This figure has clearly presented that the fibers had a trend to randomly distribute and it has no favorite orientation in the concrete matrix if the specimen has no limited boundary as described in Figure 2.9a. Otherwise, if the specimens were subjected to two or four boundaries as can be seen in Figure 2.9b and 2.9c, the fibers near the edges had a tendency to align in a parallel manner to its boundaries.

Further experimental studies accomplished by Kim and Kang [30], [31] also confirmed the much different in fibers orientation due to the casting method, thus, led to the change of the tensile strength and flexural behavior of specimens. These authors concluded that the best way to cast concrete is parallel with the tensile stress direction. The results from the dog bone shape specimens revealed that a maximum load of 45 % higher than which one from the specimens had the fibers alignment perpendicular to the tensile stress direction. However the research performed by Pansuk et al. [23] has shown the contradictory opinion. Based on the investigation of the fibers orientation numbers, he detected that the fibers had a trend to arrange themselves in the parallel direction with the concrete flow.

2.5.3 Fibers orientation determination method

There was many methods to determine the orientation of fibers by direct or indirect way, by destructive or non-destructive method. The easiest way is the visual observations during concrete casting procedure. This method can only give an idea of the real orientation of fibers.

Table 2.1 Some techniques to identify the fibers orientation

Techniques	Measurement		Method	
	Indirect	Direct	Destructive	Non destructive
Manual counting	x	-	x	-
Mechanical testing	x	-	x	-
Image analysis	-	x	x	-
X-Ray method	-	x	x	-
Impedance spectroscopy	-	x	-	x
Dielectric waveguide antennas	-	x	-	x
Electrical resistivity methods	-	x	-	x
Inductive method	-	x	-	x

The other effective method is X-ray techniques [32] which can give the accepted results of the real fibers orientation. Another method is the image analysis. The specimens were cut at some sections with the aim of seeing the orientation and dispersion of the steel fibers. By using pictures taken by a microscope or by using computerized tomography techniques, the fibers area on the cut plane could be easily obtained by the difference in the color when the concrete subjected to the flashlight, the fibers reflected it while the concrete absorbed the flashlight entirely. Based on many papers, some widely used methods to determine the fibers orientation were summarized in the Table 2.1 as shown above.

2.6 Fibers orientation and shear

2.6.1 Attachaiyawuth research [33]

This experimental study was performed at the Faculty of Engineering, Chulalongkorn University, Thailand [33]. The main objective was to study the shear properties and behavior for high strength steel fibers reinforced concrete according to the data from the push off test.

Thirty one specimens separated into four series were tested in order to investigate the parameters which will affect shear behavior and propose a cracking shear slip model to calculate the crack width and crack slip.

To study how the fibers orientation affects the shear strength, in this research, the different casting concrete methods were applied. The first one was casting concrete by flowing method and the second one was casting concrete by fall method.

A total of 31 specimens are divided into 4 series. The varying parameters in each series were the concrete compressive strength, fibers volume ratio, stirrup quantity, the angle between shear surface and principal direction of steel fibers and the angle between shear plane and stirrup. These parameters in each series were summarized in Table 2.2 as follows.

Table 2.2 Parameters in each series

	$f_c^{'}$ (MPa)	% Fibers	% Stirrup	Turbulent	Angle (θ_R)
Series 1	140	0.0	0, 1.25, 2.5	No	90°, 60°, 45°
Series 2	140	0.8	0, 1.25, 2.5	Yes	90°, 60°, 45°
Series 3	80	0.8	0, 1.25, 2.5	Yes	90°, 60°, 45°
Series 4	140	1.6	0, 1.25, 2.5	Yes	90°, 60°, 45°

The crack width and crack slip can be calculated from 3 demec points as illustrated in Figure 2.10 on specimens by equations (42) and (43) respectively.

$$W = \frac{\left(l_1^{'} - l_1\right)\cos\theta_2 - \left(l_2^{'} - l_2\right)\cos\theta_1}{\sin\theta_1 \cdot \cos\theta_2 - \sin\theta_2 \cdot \cos\theta_1} \tag{42}$$

$$\delta = \frac{\left(l_1^{'} - l_1\right)\sin\theta_2 - \left(l_2^{'} - l_2\right)\sin\theta_1}{\cos\theta_1 \cdot \sin\theta_2 - \cos\theta_2 \cdot \sin\theta_1} \tag{43}$$

where l_1 : the distance between demec point AB (before crack), $l_1^{'}$: the distance between demec point AB' (after crack), l_2 : the distance between demec point AC (before crack), $l_2^{'}$: the distance between demec point AC' (after crack), θ_1 and θ_2 : the angle between crack plane and plane AB and AC respectively.
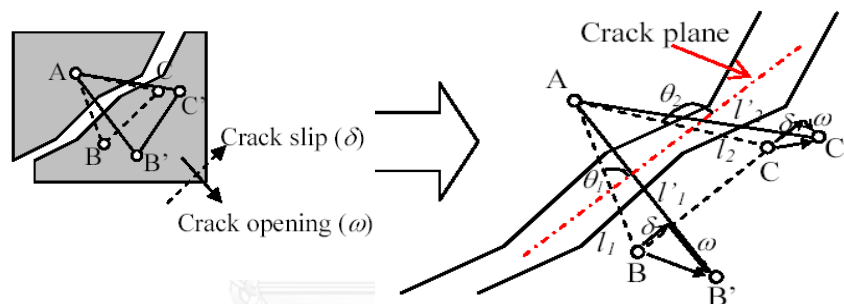
Figure 2.10 Parameters used for calculating crack width and crack slip [33]

The test results showed that the shear strength is improved by using of more stirrups but the specimens might fail suddenly. For series 1, shear strength increased about 40 % while increasing of stirrups from 1.2 % to 2.4 % and stirrups strain increased about 2 times at failure. For the series 2, 3 and 4, with the existence of steel fibers, the shear strength increased approximately 1.5-2 times while comparing to series 1. The more fibers were used the more strength specimens would get. Beside that when comparing the failure mode between the specimens with and without stirrups, the specimens without stirrups may fail suddenly. Thus, using steel fibers and stirrups together in the specimens are the most effective way to develop the shear capacity and the ductility of specimens.

Peak shear stress can be calculated by equations (44) and (45) as shown below. These two equations are specialized for specimens without stirrups and with stirrups but removed effect of stirrups respectively.

$$\frac{\tau_{peak}}{f_c^{'}} = -0.0373\theta_f + 0.2047 \tag{44}$$

$$\frac{\tau_{peak}}{f_c^{'}} = -0.0809\theta_R + 0.1207 \tag{45}$$

Fracture energy can be expressed by 2 equations as follow. Equation (46) is focused on specimens without stirrups and equation (47) for specimens with stirrups but removed effect of stirrups.

$$G_f = -0.0746\theta_f + 0.3874 \tag{46}$$

$$G_f = 0.849\theta_R + 0.1257 \tag{47}$$

After considering the test results, Attachaiyawuth concluded that principal direction of steel fibers affects not only shear strength but also crack propagation significantly. The specimens which $\theta_f = 30°$ and $60°$ show 30 % shear strength higher than specimens in which $\theta_f = 90°$ approximately. So if casting method can control the principal direction of steel fibers in advance, it will be very effective way to improve the shear behavior and shear capability of high strength steel fibers reinforced concrete members. This is the most important conclusion that we can obtained from this research.

2.6.2 Lionel and Rene's research [34]

This experimental work was performed at two locations: the University of Applied Sciences, Fribourg, Switzerland and Navier laboratory, Marne-la-Valle, France [34]. The purpose of this research was to study the interaction between the slab thickness, the tensile reinforcement percentage and the fibers volume ratio on punching shear behavior of flat slabs. Then, the tests have emphasized some influences of UHPFRC combined with steel reinforcement on flexural strength and punching shear capacity.

The tests were conducted on nineteen square slabs with the dimensions of 960x960 mm. The varying parameters were: the thickness, the fibers volume ratio, the reinforcement ratio and the reinforcement arrangement. The mix used for this study was the BCV® with a fibers volume ratio of 1 and 2 %. All slabs were casted in a same methods without any vibration machine. The concrete mixing were poured at the center of the formwork. They were removed of the formwork after 1 day and cured in the normal conditions inside the plant and covered by plastic sheet in around two weeks.

The load tests were performed on a specially designed punching test set up. The slab was supported by eight steel rods, anchored to a steel frame. The concentrated force was located at the middle of the slab and applied through a loading pad. The tests were controlled in displacement by a servo-electronic system.
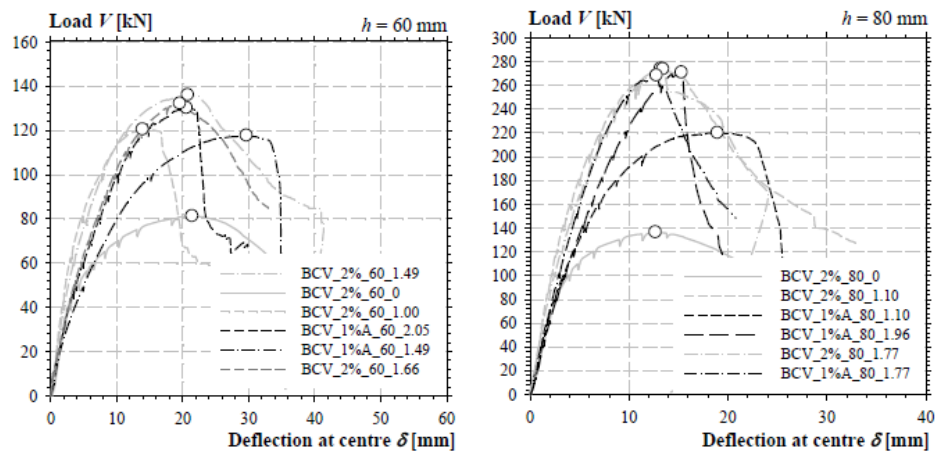
Figure 2.11 Load-deflection curves of the slabs according to the thickness [34]

Figure 2.11 presented the load vs. deflection curves of the slabs having the same thickness of 60 mm and 80 mm. The stiffness of reinforced slabs in BCV 2 % showed a higher value in the elastic-cracked stage compare to the BCV 1 % A slabs. For the slab having the same reinforcement ratio and thickness, as the fibers volume increases, the flexural and punching shear capacity increases as well.

Lionel & Rene had developed an equation to investigate the punching shear strength based on their test results. In this equation, the effect of the concrete matrix $V_{R,c}$ and the fibers distribution $V_{R,f}$ are combined to get the punching shear strength of UHPFRC slabs.

The concrete contribution is determined as the following:

$$V_{R,c} = \frac{3/4}{1+15\dfrac{\psi \cdot d}{16+d_g}} \cdot b_0 \cdot d \cdot \sqrt{f_c} \tag{48}$$

where b_0: control perimeter, determined at the distance of $d/2$ from the edges of the loading support, d_g: the biggest aggregate diameter (for UHPFRC $d_g = 0$), d: effective depth of the slab, ψ: slab rotation, f_c: compressive strength of concrete.

The fibers contribution can be calculated as:

$$V_{R,f} = \frac{1}{K} \cdot \int_{A_p} \sigma_f(w) \cdot dA_p \tag{49}$$

where K is the parameter to take account for the fibers orientation is, $\sigma_f(w)$ is the tensile stress – opening law relationship.

CHAPTER 3
EXPERIMENTAL PROGRAM

3.1 Introduction

The punching shear strength of FRC, High strength concrete and Ultra High Performance Steel Fibers Reinforced Concrete had been reviewed in the previous chapter. From the literature review, the punching shear strength was one of the design criteria to ensure the safety of the slabs and flat plates. It was affected by many parameters such as the compressive stress of the concrete, the fibers volume ratio, the slab thickness, the quantity of stirrup, the fibers distribution and orientation. Various researchers tried to study the problem about punching shear but only some of them talked about the influence of fibers distribution and orientation on punching shear capability of UHPFRC slabs. As the results, they identified that the concrete flow ability much affects the fibers orientation and enriched the concrete performance as the results.

In recent years, a great number of research in this subject has been processed, however, this problem still remains very complicated and difficult to understand and analyze. So the objectives of this experimental work is to investigate the effects of the casting direction on punching shear performance and study the punching shear behavior of the UHPFRC slabs at the ultimate failure state, then modify an equation to precisely measure the punching shear strength while considering the orientation of steel fibers. After that, the comparison between the testing data and modified equation would be given.

3.2 Experimental program

This experimental study was conducted at the Concrete and Materials Testing Laboratory, Faculty of Engineering, Chulalongkorn University. The main purposes of this experimental campaign are to examine the behavior of the UHPFRC slabs under punching failure and to determine the effects of casting direction on punching shear strength of UHPFRC slabs. The experimental was carried out on 8 square slabs which were made by UHPFRC. They were named from S01 to S08 respectively and marked on the slabs.

The first step of this study was to find the mix proportions of UHPFRC. A number of concrete cylinders and small cube were casted to achieve the mixing proportions that can give the great compressive strength, high tensile strength and good slump (in table slump flow test and V-funnel shape test) that concrete can be able to flow along the chute and fill up the mold without any vibration. After that, the main specimens, all of the eight UHPFRC slabs were casted with the same conditions and same procedure.

The UHPFRC was poured in the different way to consider the effects of fibers orientation.

The influences of steel fibers amount on the punching shear capability of the specimens were investigated on 8 slabs from S01 to S08 with different fibers volume ratio. The influences of reinforcement ratio were studied on 2 group of slabs: S01 without reinforcement and S02 to S08 with tensile reinforcement. The effects of casting direction on punching shear capacity were considered mainly in 3 position that mentioned in the next section.

The crack propagation were identified due to the change in fibers volume ratio from 0 to 1.6 %. These data would be analyzed in the Chapter 4 of this thesis. It might help in the modification of the formula to calculate the punching shear strength of the UHPFRC slabs. All features of the tested slabs and the tensile reinforcement details were given in the Table 3.1 as follow.

Table 3.1 The UHPFRC slabs information

Slabs No.	f_c (MPa)	f_{spt} (MPa)	E (MPa)	Tensile reinforcement ratio ρ (%)	Fibers volume V_f (%)	Casted positions (*)
S-01	98.0	12.5	39.34	-	1.6	Position A
S-02	97.8	8.2	40.72	2.54	0.8	Position C
S-03	98.5	8.6	53.68	2.54	0.8	Position B
S-04	87.8	7.6	37.20	2.54	0.8	Position A
S-05	99.0	12.1	47.20	2.54	1.6	Position C
S-06	86.8	11.7	31.48	2.54	1.6	Position B
S-07	96.5	11.8	38.47	2.54	1.6	Position A
S-08	91.4	5.4	45.70	2.54	-	Position A

(*) Illustrated in Figure 3.9 as below

3.3 Geometry of tested slabs

Eight square slabs with a dimension of 1000 mm in both side were casted. All of test slabs were simply supported along four sides. The slabs had the same thickness of 60 mm, tensile reinforcement ratio of 2.54 % and also the same tensile reinforcement configuration.

The varying parameters among these specimens were: the fibers volume ratio varying from 0 to 1.6 % by volume of the specimens and the fibers orientation due to the difference in casting position. The steel reinforcements were deformed bars and were positioned in a way to have an intersection at the center of the slabs. According to the reinforcement ratio, the slabs had reinforced with $\phi 12$ mm in diameter in each direction

with the equally space of 100 mm. The size and reinforced arrangement of the slabs were shown in detail in Figure 3.1.
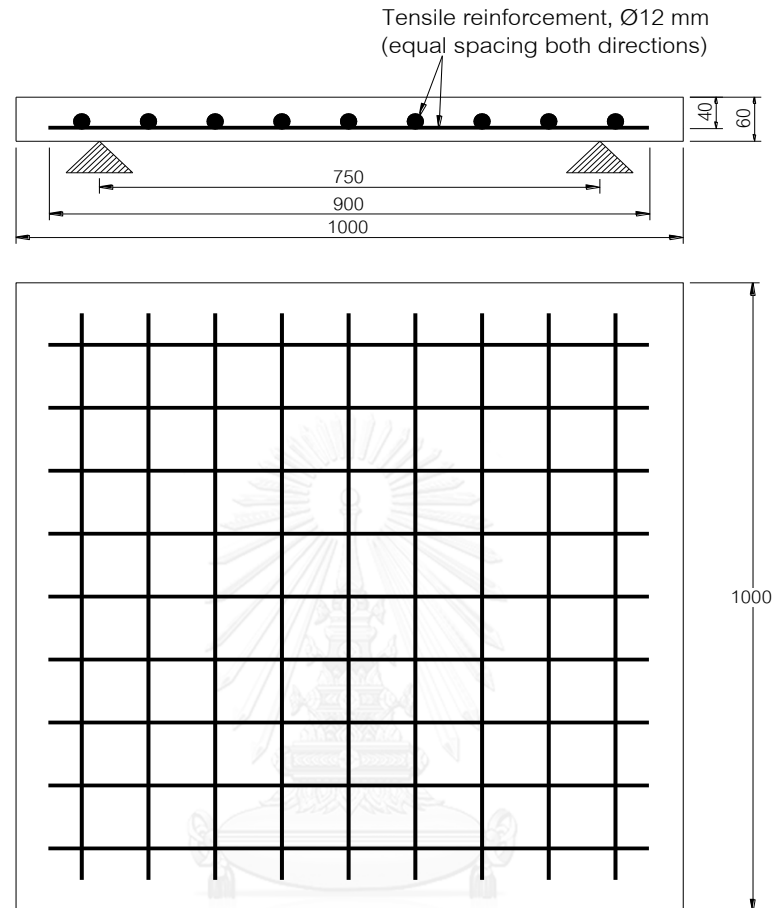
Figure 3.1 Dimensions and reinforcement details

3.4 Materials

The mix design using in this study was similar to the mix design performed by Attachaiyawuth [33] which was based on the typical mix proportions for UHPFRC including cement, sand, silica fume, superplasticizer, water and steel fiber. All of these materials were available on the Thailand local market except steel fiber were imported from Dramix material company. The following components were used to generate UHPFRC.

3.4.1 Cement

Ordinary Portland cement (type I) of a local brand TPI was used in this experimental work. Typical chemical components and the properties of the cement were presented in Table 3.2 as below according to ASTM C 150 type I [35].

Table 3.2 Cement standard requirements

Chemical requirement	Specifications limit	Test results
SiO_2 (%)	-	20.6
Fe_2O_3 (%)	Less than 6.0	3.3
Al_2O_3 (%)	Less than 6.0	4.4
CaO (%)	-	62.9
MgO (%)	Less than 6.0	2.2
SO_3 (%)	Less than 3.0	2.7
Na_2O (%)	-	0.19
K_2O (%)	-	0.50
Loss on ignition (LOI) (%)	Less than 3.0	2.7
Insoluble Residue (IR) (%)	Less than 0.75	0.27

3.4.2 Silica fume

The silica fume used in this research was made by Elkem a bluestar company. The type was Microsilica Densified Grade 920 conforms to ASTM C 1240-14. It weighed 20 kg per pack and the typical components were shown in Table 3.3 below.

Table 3.3 Silica fume specifications

Chemical and physical requirement	Specifications limit
SiO_2	Minimum 85 %
H_2O	Maximum 3 %
Loss on Ignition	Maximum 6 %
Specific Surface Area	Minimum 15 m^2/g
Pozzolanic Activity Index, 7 days	Minimum 105 % of control
Bulk density	500-700 kg/m^3

3.4.3 Sand

The river sand was used for the mix of UHPFRC in this study. It was produced by a local brand named CPAC. It was sold on the market in 25 kg bags with the grain size is not over 1 mm. Sand was taken out from the bag and let it dry naturally under the room temperature and normal conditions to avoid the additional moisture of the sand in the package which can increase the water/ binder ratio and influence to the properties of the UHPFRC mix.

3.4.4 Superplasticizer

The water reducing admixture used in this experimental study is a MasterGlenium®
SKY 8320 made by BASF chemical company. This is a new generation of great range
water reducing admixture which includes polycarboxylate ether polymers (PEP). It is
particularly designed for well concrete mixture where the slump preservation, high and
very high strength and good performance in term of durability are prerequisite in high
temperature conditions. The ability to work with low water /cement ratios and still get
extended slump retention permits for the production of high quality concrete. The
typical mechanisms of SKY 8320 that it has been produced based on a unique
polycarboxylate ether polymers with long lateral chains which can provide a flow able
concrete while the water demand is significantly reduced.

3.4.5 Steel fibers

Figure 3.2 showed the steel fibers type which was used in this study. This type of fibers
was Dramix OL 13/0.2 which is manufactured by Bekaert Corporation. This fibers have
a length of 13 mm and a diameter of 0.2 mm. It is a short straight discrete type of steel
fiber.

Figure 3.2 Steel fibers used in UHPFRC slabs

The steel fibers used in this study have an aspect ratio of 65 and the ultimate tensile
strength is over 2000 MPa. The properties of Dramix OL 13/0.2 steel fibers were
summarized in Table 3.4.

Table 3.4 Dramix steel fiber specifications

Fiber type	Length (mm)	Aspect ratio	Shape	Minimum tensile strength (MPa)
Dramix OL 13/0.20	13	65	Straight	2000

3.5 Mix design

A numbers of trial mix had been casted in order to get the suitable mix design of UHPFRC for this study which had to be able to flow along the chute and give the accepted compressive and tensile strength. Figure 3.3 showed the table slump flow and V-funnel test of the mix which was used in this study. On average, the slump spread of the mix was around 700 mm and the V-funnel test time was around 20 seconds.

Figure 3.3 Slump flow test details

The water/binder ratio using in this study was 0.21, the silica/binder ratio was 0.072 and the additive/binder ratio was 0.02. The components of the mixture are described in the Table 3.5. The target strength of the concrete under compression is around 100 MPa. The target tensile yield strength of the concrete was around 10 MPa.

The steel fibers volume ratios of these slabs are varying from 0, 0.8, 1.6 % respectively and the proportion of sand in the mixture was changed with the steel fibers volume ratio accordingly.

Table 3.5 Mixed proportions (for 1 m3 of UHPFRC)

Cement	Sand	Silica fume	Steel fibers	Super plasticizer	Water
953.86	varying	74.01	varying	20.56	varying

3.6 Steel reinforcement

Steel reinforcement arrangement for the slab specimens was based on design code provided by ACI 318-11 2011. The steel reinforcement using for this experimental study was 12 mm in diameter. The steel reinforcement was a constant parameter in this study. For each slab, total 18 steel bars of 900 mm length were used. The steel

reinforcement were placed in two directions of each specimen with exactly the same arrangement in which consisted of a regular square mesh, placed in a way to have the rebar positioned at the center of the slab.
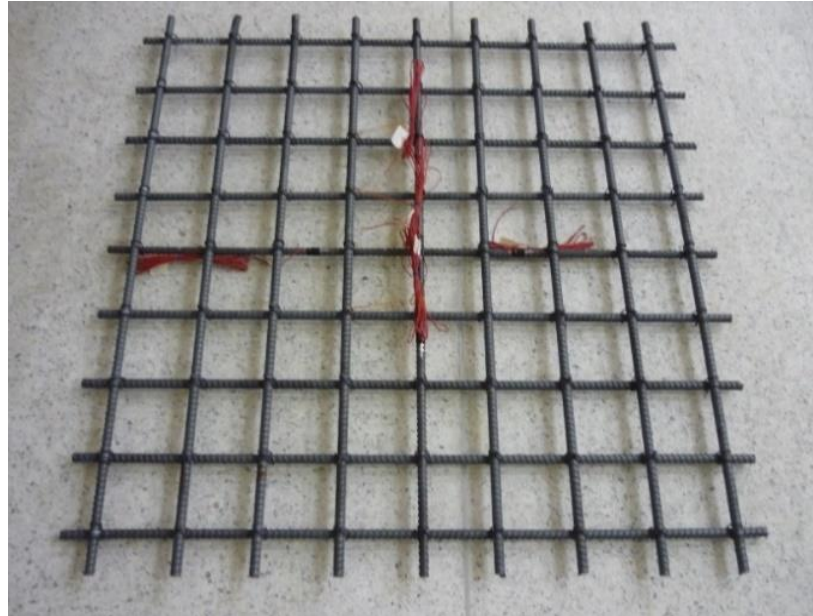
Figure 3.4 Typical steel reinforcement configurations

The tensile yield strength of steel rebar was around 250 MPa. In order to obtain the strain of steel rebar, for each slab, 5 strain gages were tightly attached to the middle bar of seven slabs in two ways. Before mounting the strain gages to the steel bar, the outside surface was crushed with a masonry grinding pad to guarantee a flat surface for well bonding. The steel reinforced arrangement was detailed in Figure 3.4 as above.

3.7 Concrete properties

To obtain the UHPFRC material properties of such as compressive strength, maximum tensile strength from splitting tensile test, each particular mixture proportions of slabs had the representative cylindrical specimens for testing its material properties. The cylinders had the standard dimensions of 150 mm in diameter and 300 mm in height. The samples were tested at the age more than 28 days after casting process.

In compression test, two strain gages were tightly bonded to each cylinder for measuring the lateral and longitudinal strain to achieve the stress-strain curve of UHPFRC material. The compressive test was based on the ASTM C39 [36] standard test method by using the AMSLER 500 tons capacity machine as presented in Figure 3.5. The compressive stress, maximum tensile yield strength and the elastic modulus of concrete were introduced in the Table 3.1 as shown in the previous section.

Figure 3.5 - Cylinder compressive test set up

There were two method to obtain the tensile strength of concrete in general: direct tensile test and indirect tensile test set up including splitting tensile test and bending test on unnotched specimens. Each method had their own advantages and limitations associated with the influence of size factor and boundary conditions of the experiment set up. For this study, splitting tensile test were adopted to measure the tensile capability of UHPFRC specimens.

Normally, standard splitting tensile test, so-called the Brazilian test, is the easy and much used method to obtain the tensile strength of concrete mixture. It is normally conducted on standard cylinders dimensions of 150x300 mm (diameter and height of the cylinders, respectively). These dimensions are appropriate to create representative samples for most types of concrete including conventional concrete, FRC and UHPFRC. However, in some case, splitting tensile test had a disadvantage while comparing to the direct tensile test that it did not offer the appropriate results of the post cracking behavior of the material. It only provided the measure of tensile strength only.

The splitting tensile test for this study was based on the ASTM C 496 [37] standard test method by using the compression machine type TMC 300 tons capacity. The configuration of the splitting tensile test was shown in Figure 3.6 as below. The splitting tensile test outcomes had been summarized in Table 3.1 as illustrated in the previous section.

Figure 3.6 Cylinders splitting tensile test set up

The modulus of elasticity might be calculated by Equations 50, 51 or 52 reported by Ma et al. [38], Graybeal [39] and ACI 363R [40], respectively.

$$E = 19000 \sqrt[3]{\frac{f_c^{'}}{10}} \tag{50}$$

$$E = 3320 \sqrt{f_c^{'}} + 6900 \tag{51}$$

$$E = 3840 \sqrt{f_c^{'}} \tag{52}$$

In this study, the stress-strain relationship gained from the cylinders test were applied to calculate the chord modulus of elasticity of the UHPFRC slabs. This calculation procedure was based on ASTM C 469 [41] as can be seen in Equation (53).

$$E = (\sigma_2 - \sigma_1) / (\varepsilon_2 - 0.00005) \tag{53}$$

where σ_2 is the stress corresponding to 40 % of the ultimate load of the concrete, σ_1 is the stress corresponding to a longitudinal strain of $\varepsilon_1 = 0.00005$ and ε_2 is the longitudinal strain produced by σ_2. The results of chord modulus of elasticity were shown in Table 3.1 as above.

3.8 Mixing procedure

The casting procedures were based on the mixing protocol derived from the research of Lee and Crisholm [42] and observed in the casting procedure of all specimens. When concrete were mixing, the time was measured and noted for later works. In fact, for the normal laboratory condition and room temperature, the times for concrete mixing in this study were followed as mention in Table 3.6 as below.

Table 3.6 Time procedure for UHPFRC mixed

Mixed Procedure	Accumulative time (in minutes)
Dry mixing	0 - 2
Add 87% of water and 50% of super-plasticizer	2 - 5
Stop mixing	5 - 7
Continue mixing	7 - 15
Add remaining water and super-plasticizer	13
Add steel fibers	15
Stand up	15 - 25
Finish mixing and cast the specimens	25 - 30

3.9 Formwork and supporting frame

The steel formwork was used in this study. It was combined of some parts of steel stick together by the nail and can remove easily in order to reuse for the next slab. The size and the arrangements were detailed in Figure 3.7.

a)   b)

Figure 3.7 Slab formwork a) without rebar b) with rebar

The supporting frame consisted of 4 steel columns H 100x100 mm which were connected together by 8 steel beams: 4 steel beams H 100x100 mm at the bottom and 4 steel beams H 200x100 mm at the top of the supporting frame. All of the components were connected by electric welding method.

**Figure 3.8** Slab supporting frame

To symbolize the simply supported, 4 steel beams L 100x100x7 mm were welded on the top of 4 steel beams H 200x100 mm mentioned above. The details of the supporting frame were shown in Figure 3.8.

3.10 Casting procedure

The casting method was the key point for the fibers orientation. In this study, three positions were proposed. Three positions were named as Position A, B and C. Position A was at the center of the slab, position B was at one side of the slab while position C was at one of four corner of the slab as displayed in Figure 3.9. The concrete spread out from the pouring location until it full filled the formwork. Due to the geology symmetry of the slabs so the location could be chosen at any side or corner of the slab. The positions were marked on 8 slabs to differentiate among them.

In order to ensure good casting repeatability and align the fibers orientation before coming to the mold, a chute was used in this research. It was made by steel and made an inclined angle of 20 degree with respect to the horizontal plane. The chute length was around 1.6 meter long.
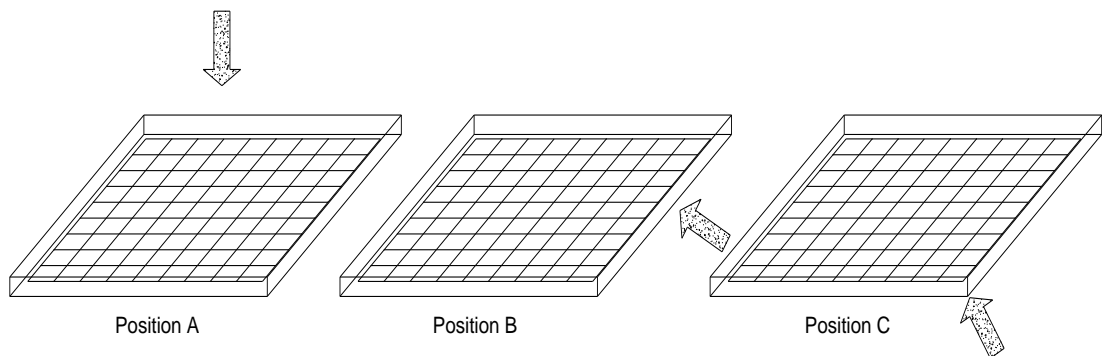
Figure 3.9 The pouring concrete positions

The casting procedure were described in the Figure 3.10 as shown above. The mold and the chute were placed at the desired positions before the mix procedure finished (Figure 3.10a). The formwork was put on the hand lifter in order to move the slabs to the store room after. Let the concrete flowed along the chute until it came to the formwork and filled it full as can be seen in Figure 3.10b and 3.10c.

a)   b)   c)
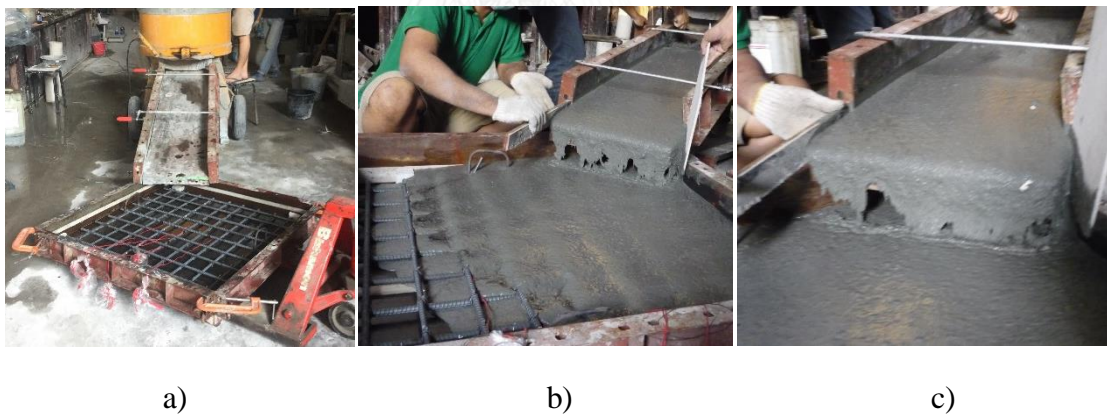
Figure 3.10 Casting method in this study (at corner position)

3.11 Curing process

The specimens were removed from the mold after 1 day of casting. Then the slabs were moved to the available places while the cylinders were placed in the tank fully fill with the water. The samples were placed in the concrete laboratory under an average temperature of $25°C$ and normal curing conditions without heat treatment. Figure 3.11 presented the slabs at the stored room.

**Figure 3.11** UHPFRC slabs after removing the mold

3.12 Equipment

The punching shear tests were conducted at the Concrete Laboratory of Faculty of Engineering, Chulalongkorn University. The specimens had been tested under the punching shear test setup which was designed for this study.

Due to the symmetry of the slab, five linear variable differential transducers (LVDTs) were installed to determine the vertical deflections of the specimens, one LVDTs was attached at the middle point of the bottom surface of the tested slab, another four LVDTs were positioned on the loading surface in which two LVDTs were at the quarter of span of the slabs and the other two were at the corners to get the movement of the slab corners.

Before the test, the LVDTs were checked the accuracy when measuring the displacement by using some small glass plates. The loading machine was also checked how well it measures the applied load to the specimens. After that, all equipment were connected to the control system. The LVDTs were placed in vertical direction and were attached to the supporting frame through a support link. The slabs were placed directly on the supporting frame and assured that the concentrated load was at the center of the slabs. Figure 3.12 showed the LVDTs configurations and the supporting frame set up for this study.
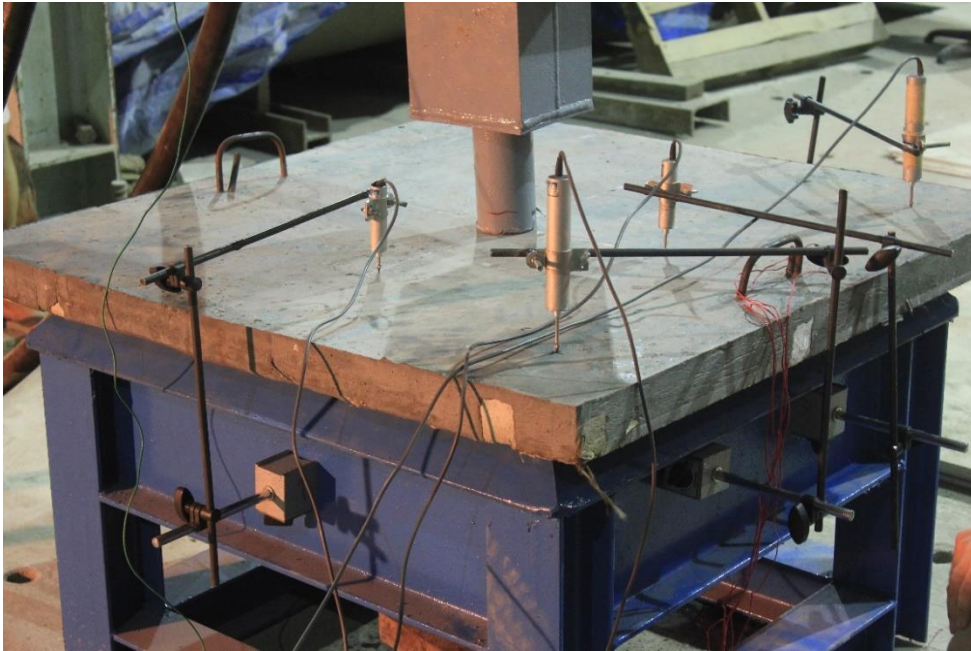
Figure 3.12 LVDTs placement configuration
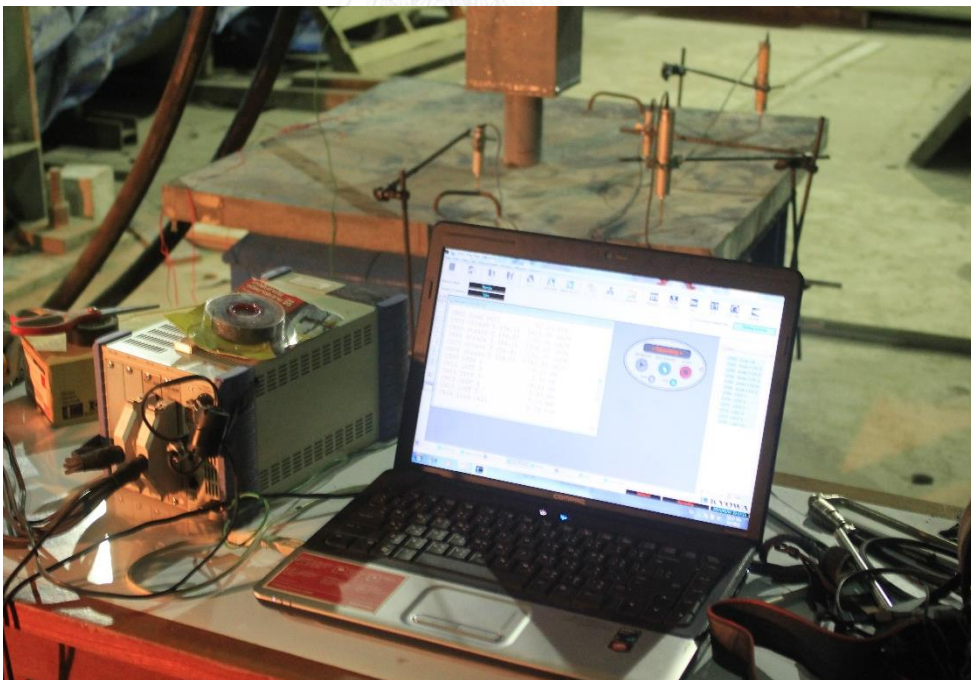
Figure 3.13 Testing control system

The LVDTs and strain gages on steel reinforcement were connected to a control system as shown in Figure 3.13. The results were recorded by a data logger model EDX-100A produced by Kyowa Inc. The data was recorded at every 0.1 second until the failure of each slab.

3.13 Punching shear test setup

The slabs were loaded by a 200 tons capacity hydraulic jacks. The slabs were simply supported along four sides and free to move at four edges. The load was applied gradually with the increments of 5 kN until the ultimate failure of the slabs was observed. At each step, the yield line pattern and crack opening were observed and the photos of crack line were taken. The compressive test of cylinders were conducted at the same days corresponding with the slabs testing. All equipment and machine were shown in Figure 3.14 as shown below.

Figure 3.14 Punching shear test setup of UHPFRC slabs

After the punching shear test finished, the specimens were cut at some positions on the failure cone to see the real distribution and orientation of fibers. Image analysis is a well-built and trusted method and is usually applied in analyzing the dispersal and direction of steel fibers in UHPFRC and FRC in general. Principally, micrograph were taken from the cross section of the specimens and several fibers diffusion can be estimated such as segregation, orientation, clumping, etc. This study focus on the fibers orientation. On the representation selection of tested specimens, orientation of the steel fibers was displayed and presented visibly its trend within the concrete matrix. To obtain the information of distribution and orientation of fibers, manual counting was first performed in this study. The result would be discuss in the following section.

CHAPTER 4
TEST RESULTS AND DISCUSSIONS

4.1 Introduction

This section gives the results of all the tests which were conducted in this study including: the load-deformation curves of the tested slabs, the compressive strength, the maximum tensile strength of the UHPFRC, the crack propagation, the failure modes of UHPFRC slabs, the critical perimeter, the punching shear cone size and the fibers orientation and distribution on the cut plane of the slabs.

4.2 Compressive strength of UHPFRC

Compression testing of cylinders was the primary method used to decide the compressive strength of the UHPFRC. The results of the tested cylinders were shown in Figure 4.1 as below.
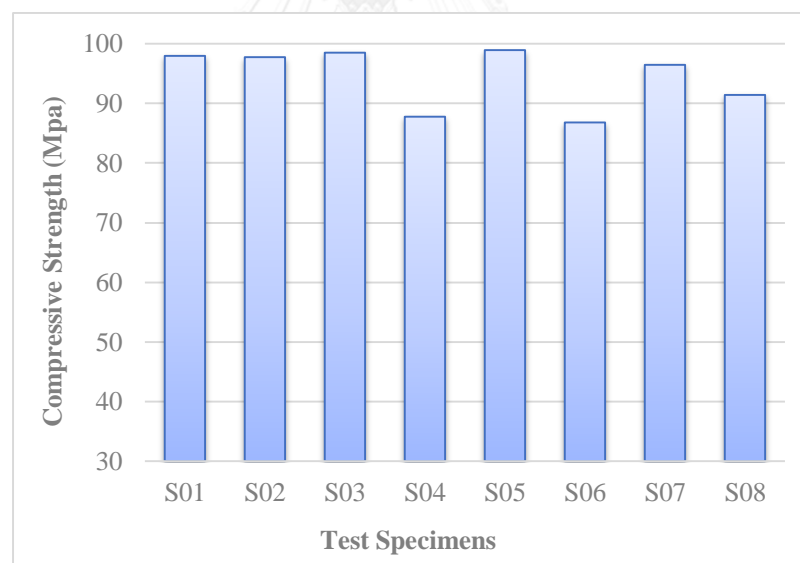
Figure 4.1 Compressive strength of test specimens

Figure 4.1 showed that the steel fibers have no considerably effects on the compressive strength of the specimens. Specimen without fibers (S08) had the compressive strength of 91.4 MPa while specimens with 0.8 % and 1.6 % of steel fibers showed a slightly higher in compressive strength from 96 to 98 MPa, respectively. For specimens S04 and S06, the steel fibers even reduced the compressive strength of UHPFRC specimens.

There were two types of failures of cylinders with and without fibers under compression due to the effect of steel fibers in the UHPFRC mixture as shown in Figure 4.2. After the development of the cracks, the bridging effects of steel fibers can help the matrix to resist extra forces so that the failure mode of the cylinders with fibers were more ductile as can be observed in Figure 4.2a while comparing to the brittle failure mode of the cylinder without fibers, which clearly illustrated in Figure 4.2b.


a)   b)
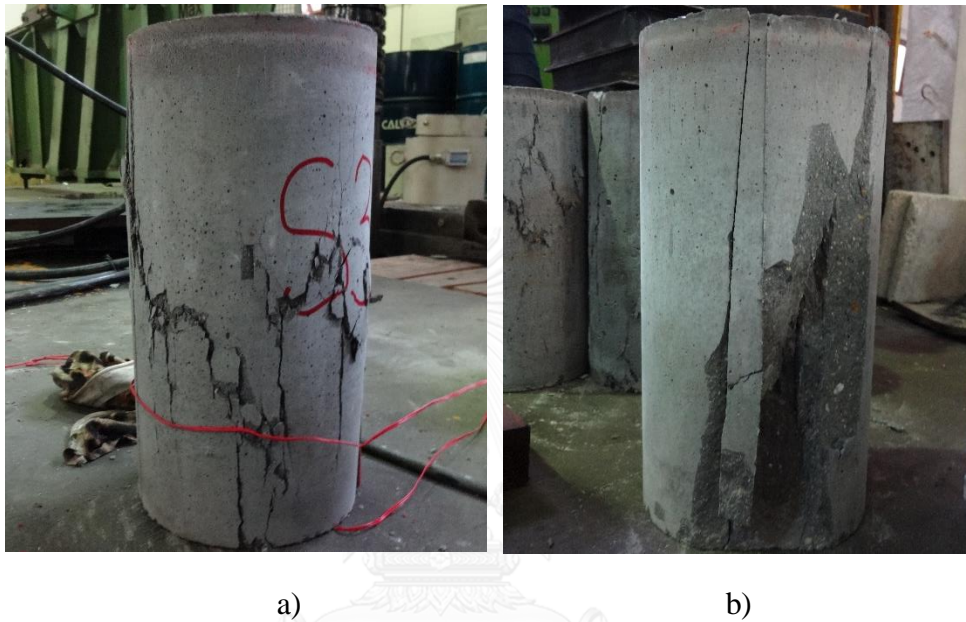
Figure 4.2 Typical failures of cylinder under compression

4.3 Splitting tensile strength of UHPFRC

Splitting tensile test was the indirectly methods to measure the tensile strength of concrete by loading a cylinder under compression force through a straight line load applied along its length. This test was conducted by a standard concrete compression testing machine type TMC 300 tons capacity with the specific requirements of the hinged bearing that loads the cylinder. The loads at which the cylinders failed were recorded during the test. Based on ASTM C 496, the maximum tensile stress can be calculated by equation (54) as shown below. The results were summarized in Table 1 as shown in previous section.

$$f_{spt} = \frac{2P}{\pi l d} \tag{54}$$

where f_{spt} is the maximum tensile strength, P is the maximum applied load to the cylinder, l is the length of cylinder and d is the diameter of the cylinder.
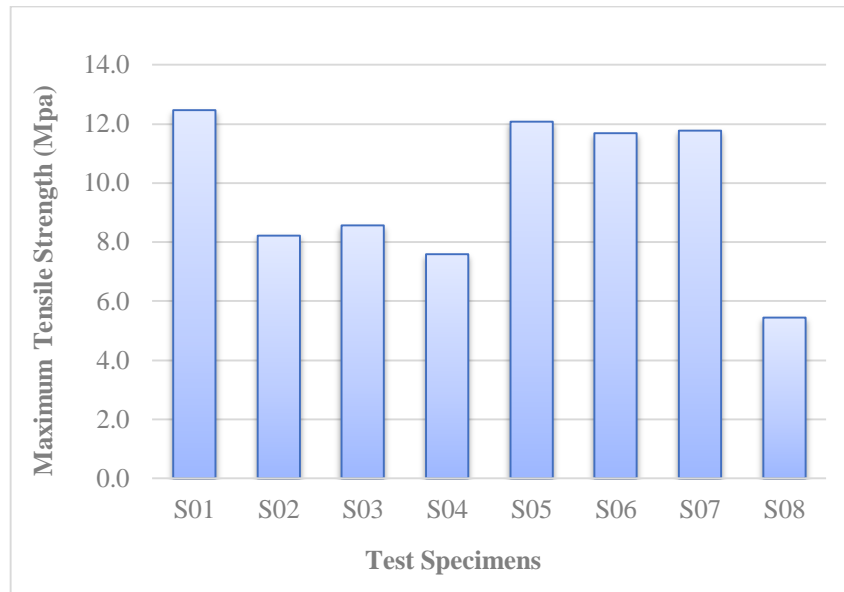
Figure 4.3 Maximum tensile strength of test specimens

The typical failure modes of the specimens under splitting tensile test were shown in Figure 4.4. The results showed clearly how well the fibers effect the failure mode of the cylinders. The cylinder without fiber (S08) has a maximum tensile strength of 5.4 MPa, while the cylinders with fibers show a significantly increase in tensile stress about 44 % with 0.8 % of steel fibers and 118 % with 1.6 % of steel fiber comparing to that value of cylinder without fibers. In addition, the fibers also change the failure mode of the cylinders from the brittle of specimens without fibers (Figure 4.4a) to ductile behavior of specimens with fibers (Figure 4.4b) thanks to the connecting behavior of steel fibers which reduce the macro cracks and increase the micro cracks.


a)   b)
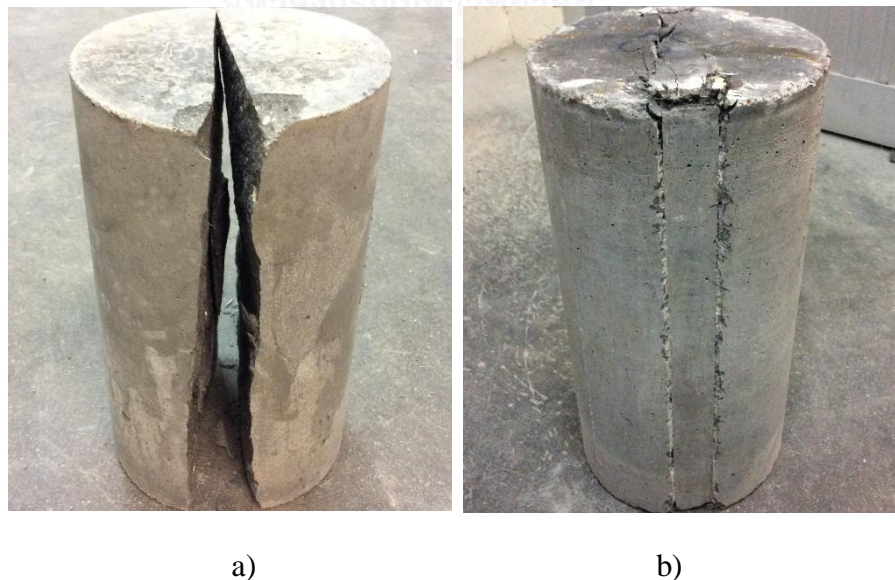
Figure 4.4 Typical failure modes of the cylinder under splitting tensile test

4.4 Load-Deformation behavior

The relationship between the applied load and the deformation at the middle of the tested slabs, obtained from the experimental data, was plot on the graph as shown in Figure 4.5 for all tested slabs from S01 to S08.

From Figure 4.5, the loading-deflection behavior of the tested slabs with and without steel reinforcement can be achieved from the beginning of the test until the load reached to the peak value (failure load) due to the test arrangement. The curves may divide into two parts based on the observations of the crack development.

In the first part, before the observations of the first cracks, the behavior was approximately elastic linear and the curves were closed to each other due to the similar thickness so the stiffness of the tested slabs were quite similar at the first stage. Whenever the tensile strength of the concrete matrix was reached, the first cracks appeared at the center of slab, closed to the loading area. After that, the stiffness lost and reduced progressively following by the development of the cracks.
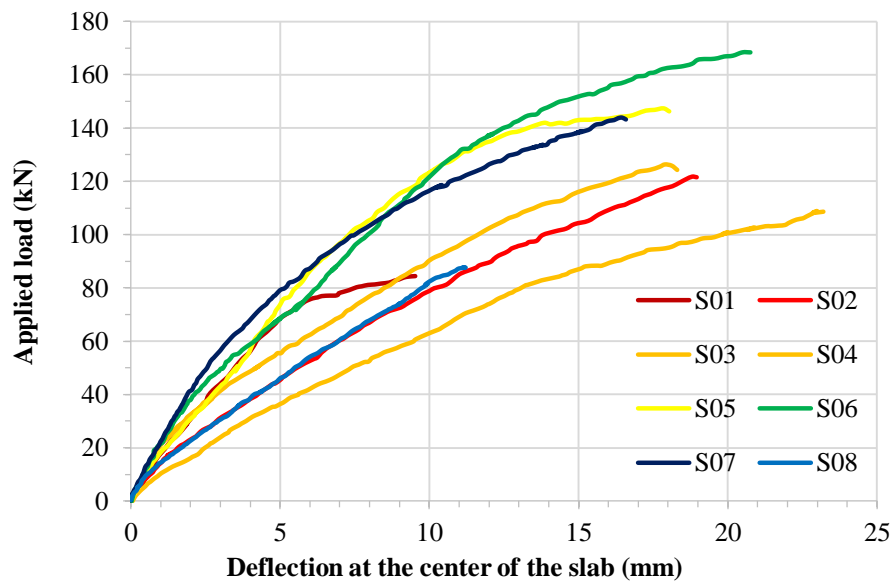
Figure 4.5 Load-deflection curves of tested slabs

For the slabs without reinforcement but containing steel fibers in the component (slab S01), after the development of the first cracks, the fibers were activated and help the concrete matrix to resist the forces and reduce the cracks width. Until the fibers were pull out from the concrete, the cracks propagated and developed toward the ends of the slabs. Slab S01 showed a flexural failure as can be displayed clearly in Figure 4.10 and Figure 4.11. After the ultimate failure, no punching shear cones were created for this slab.

For the slabs with reinforcement but no steel fibers in the matrix (slab S08), once the appearance of the first cracks, the steel reinforcement started to resist forces. The steel reinforcement can only resist forces until the tensile yield strength reached the limit value and then the stiffness decreased significantly.

The other slabs which contained both steel reinforcement and steel fibers showed the higher results in load resistance due to the cohesive effects of reinforcement and steel fibers. Consequently, the cracks propagated to the end of the slabs, then the critical shear cracks developed leading to the punching shear failure of slabs.

From the experimental results, the punching shear failure load increased from 87 kN for slab S08 to 168 kN for slab S06. The punching cones were created after the ultimate failure load.
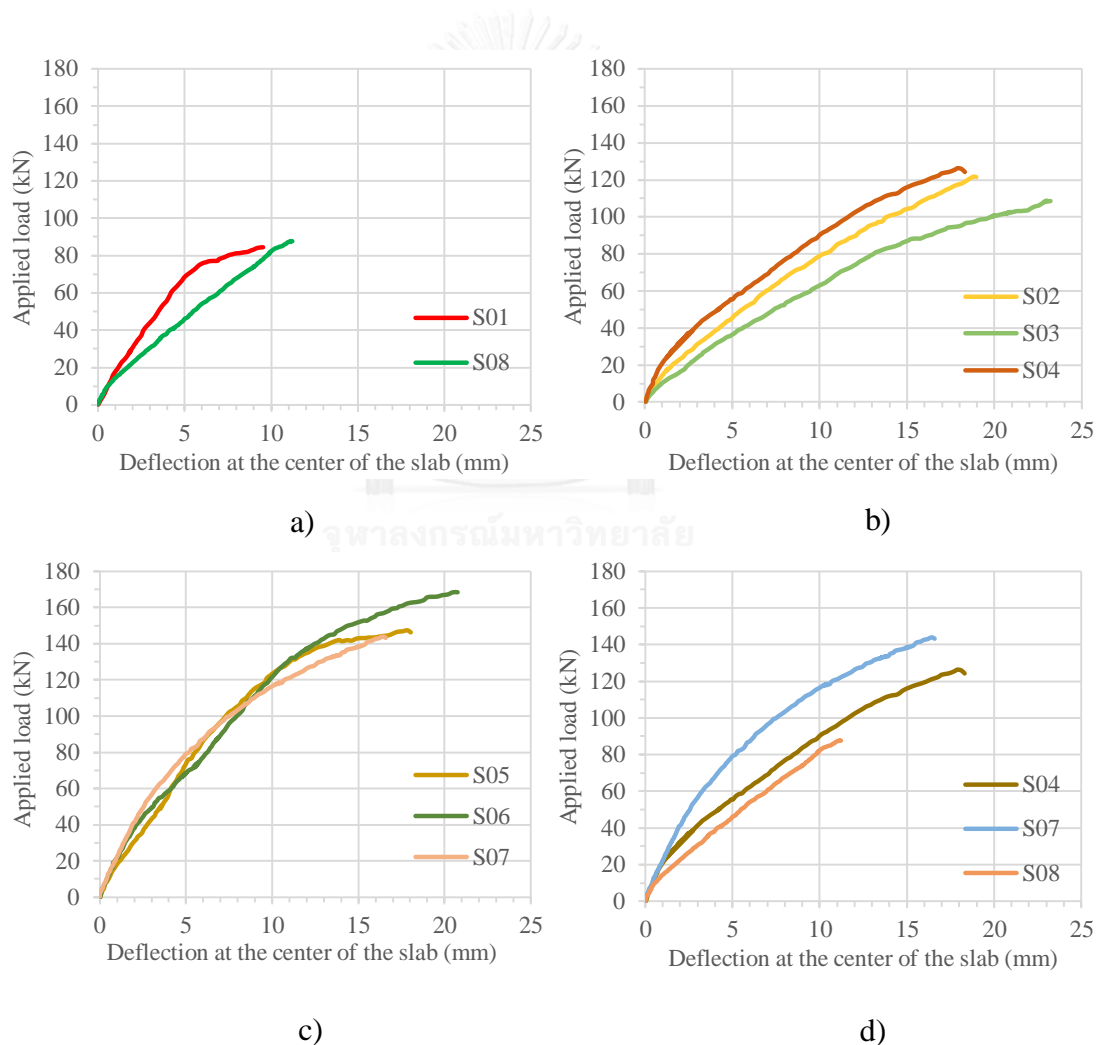
Figure 4.6 Load-deflection curve according to slab thickness

In order to highlight the influence of the steel reinforcement and the steel fibers to the properties of UHPFRC slabs, the eight slabs were divided into three groups. The load-deflection curves of these groups were plot separately on some graphs which were showed in Figure 4.6.

To emphasize the effects of steel fibers volume ratio and the concrete casting direction, the 6 slabs were categorized in two groups of the same fibers volume ratio, group 2 of three slabs: S2, S3, S4 with 0.8 % of steel fibers and group 3 of three slabs: S5, S6, S7 with 1.6 % of steel fibers.

These load-deflection curves were showed in Figure 4.5b for group 2 and Figure 4.5c for group 3. For these group, the steel fibers increased the failure load by 37 % and 76.83 % in average, respectively while comparing to that value of group 1. The load and deflection values of the tested slabs were showed in Table 4.1 as below and the failure load comparison of tested slabs were given in Figure 4.6.

**Table 4.1** - Load and deflection of the tested slabs

Group	Name	First crack load (kN)	First crack deflection (mm)	Failure load (kN)	Failure load deflection (mm)
1	S01	18.47	1.15	85.91	9.34
	S08	18.76	2.83	87.31	13.81
2	S02	26.25	2.54	121.92	14.99
	S03	23.27	2.94	108.27	27.46
	S04	27.13	1.53	125.80	15.24
3	S05	31.79	2.22	147.55	17.70
	S06	36.36	1.94	168.90	19.45
	S07	30.70	1.51	143.03	15.51

From Figure 4.6, the effects of casting direction on punching shear load of slabs in group 2 were clearly demonstrated. Slab S04 with the concrete casting position at the middle of the slabs (position C) showed the best performance between 3 slabs. It could be explained by the orientation and distribution of fibers in matrix. Slab S04 which was casted at the middle of the slab, the fibers tended to flow and distribute in all directions. It could help the slabs to resist more forces when the load was applied continuously until the slabs totally failed.

For slab S02 and S03, the fibers might have a tendency to align along the concrete casting direction then the effects on punching shear strength of these slabs were less than in the case of slab S04.

But for group 3, the effects of casting direction on punching shear load were not clearly illustrated. It might be caused by the high volume of steel fibers in the concrete matrix combining with the 'blocking effect' of the steel reinforcement could eliminate the

advantages of each other and then the difference in casting direction were not noticeably seen between these slabs.
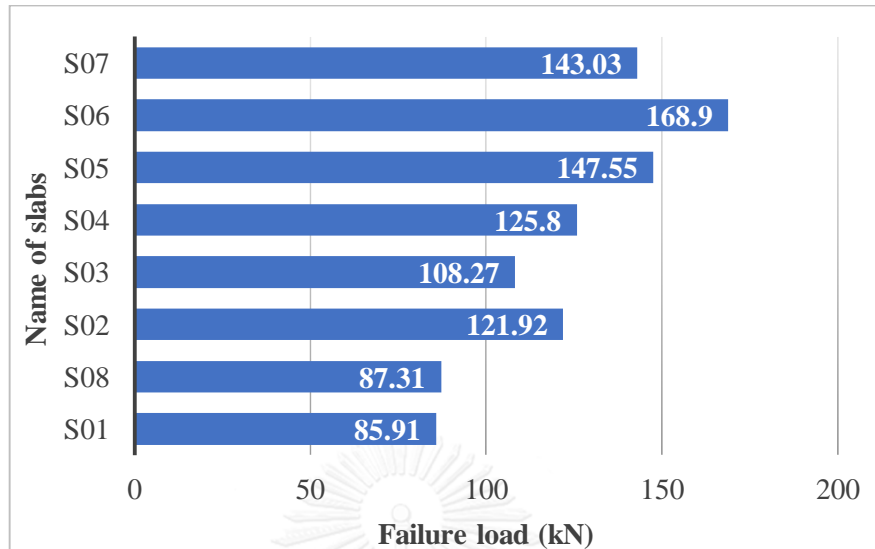

Figure 4.7 Failure load of tested slabs

4.5 Modes of failure and cracks patterns

As mentioned above, there were two types of failure mechanism for the tested slabs: flexural and punching shear. The slabs were designed to fail in punching shear mode so that the flexural failure was moderated and happened only for the slab without steel reinforcement.

A punching shear failure was characterized by a brittle failure which happened near the loading area or support column when the slab failed to carry more forces followed by the development of punching shear cone at the ultimate failure load. The typical punching shear failure on the tensile face was shown in Figure 4.9.

All of the tested slabs excluding slab S01 (slab without steel reinforcement) failed in punching shear mode as pictured in Figure 4.8, Figure 4.11 and Figure 4.12. The failure started with the flexural cracks on the tensile face near the loading position and as the load increased, the cracks propagated heading to the end of the slabs.

The more fibers were added to the concrete matrix, the less number of flexural cracks were created while the higher punching shear resistance of UHPFRC material. This phenomenon could be observed clearly while looking the numbers of flexural cracks created on the tensile surface of the tested slabs. Figure 4.8 showed the differences of the cracking pattern on the tensile face of total 8 slabs as shown below. In this figure, the symbol S-XX/X was represented for each tested slab. The two letters XX means the number of the slab and the last letter X means the casting position of this slab (e.g. S01/A: slab number 01 and casting position at the center of this mold).
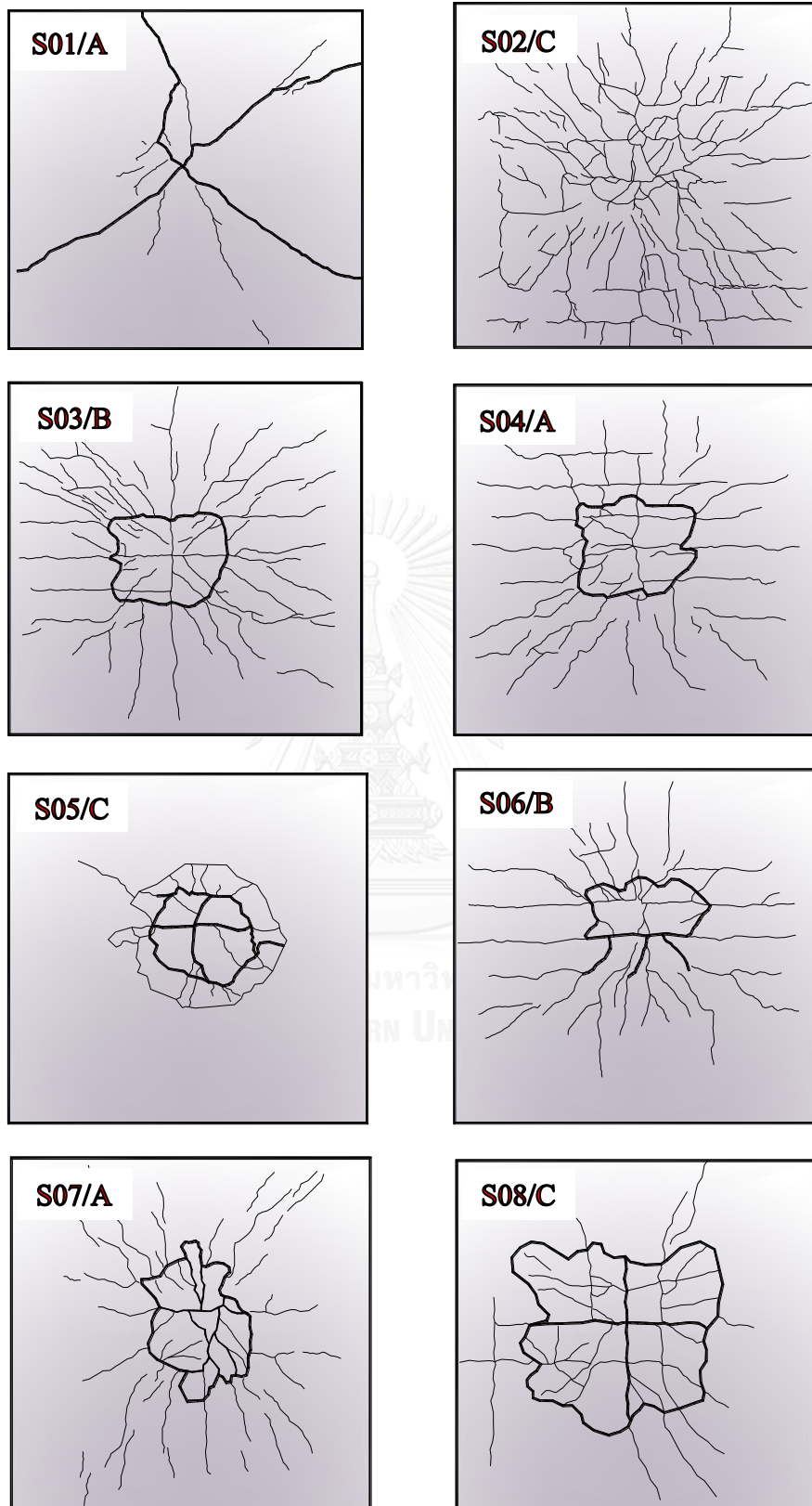
Figure 4.8 Cracks pattern of all tested slabs
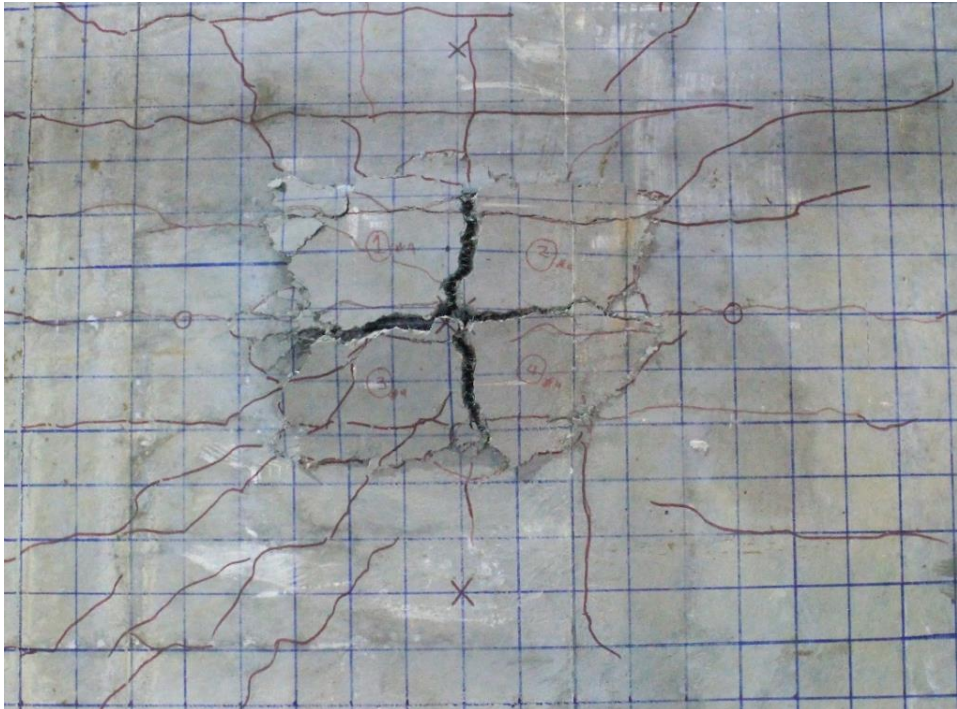
Figure 4.9 Typical punching shear failure of UHPFRC slabs with steel fiber and steel reinforcement
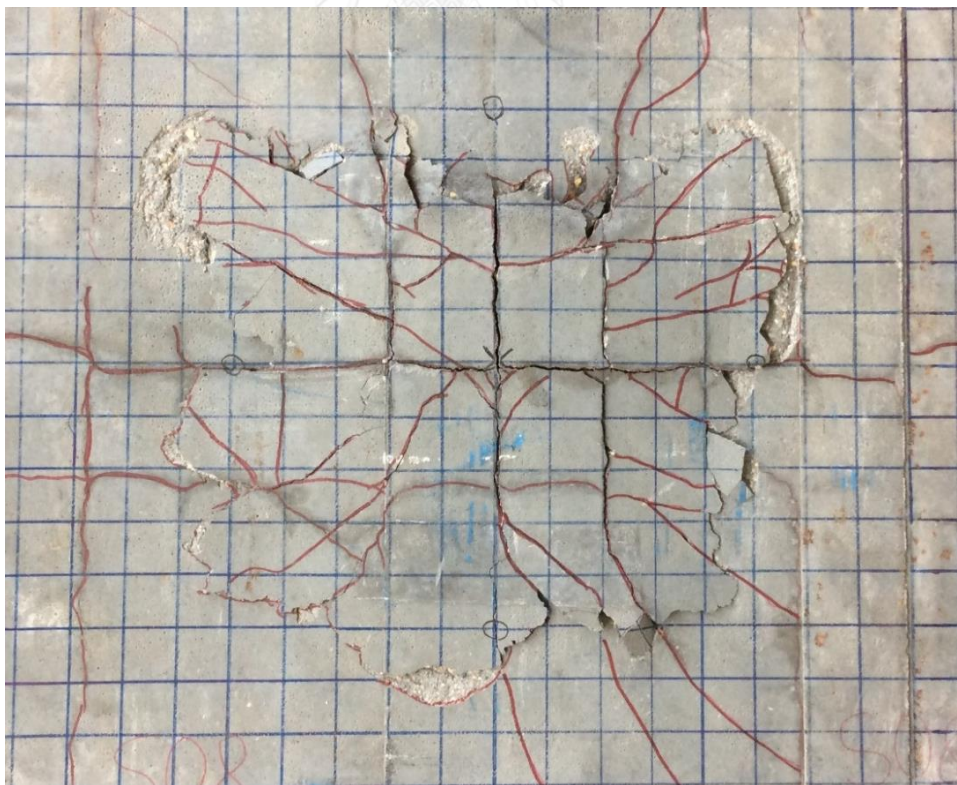
Figure 4.10 Typical punching shear failure of UHPFRC slabs with steel reinforcement and without fiber

The cracks patterns of all tested slabs showed clearly that the steel fibers could change the behavior mechanisms of the UHPFRC slabs. For slabs S08 without the steel fibers, the failure mode was characterized by the big punching shear cone and considerably damaged on the tensile face. The huge cracks developed near the critical shear perimeter and led to the failure of the slab. This was caused by the early yielding of steel reinforcement that shifted the critical shear area far away from the loading location of this slab. The typical punching shear failure of slab reinforced by steel rebar but no fibers reinforced was shown in Figure 4.10 as above.

For the slab S01 without reinforcement but with fibers in the matrix, it showed the flexural failure behavior at the ultimate load as can be observed in Figure 4.11 and Figure 4.12. The cracks started from the loading area and run until the edges of the slab. Fibers could help the matrix to resist the forces until the fibers were pull out from the concrete or were broken. Without reinforcement, this slab could resist only a haft of load while comparing to that value of slabs with both reinforcement and steel fibers in the matrix. For this case, fibers reduced the numbers of cracks and no punching shear cone was obtained at the final stage of the test.
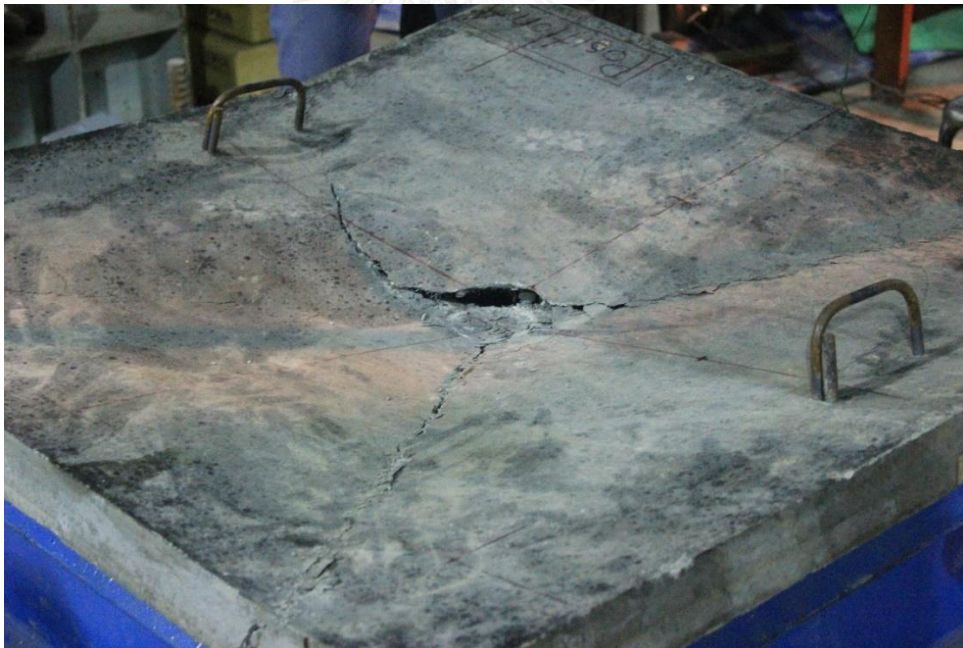
Figure 4.11 Loading face of slab S01 failed in flexure

For slab S05, the failure was pure punching shear at the ultimate load due to the formation of the punching cone without the flexural crack outside the critical perimeter. For slab S02, the critical shear crack could not be recognized by the bear eyes because the failure of this slab starts with the splitting of the concrete cover and then transferred to punching shear failure mode as showed in Figure 4.8.
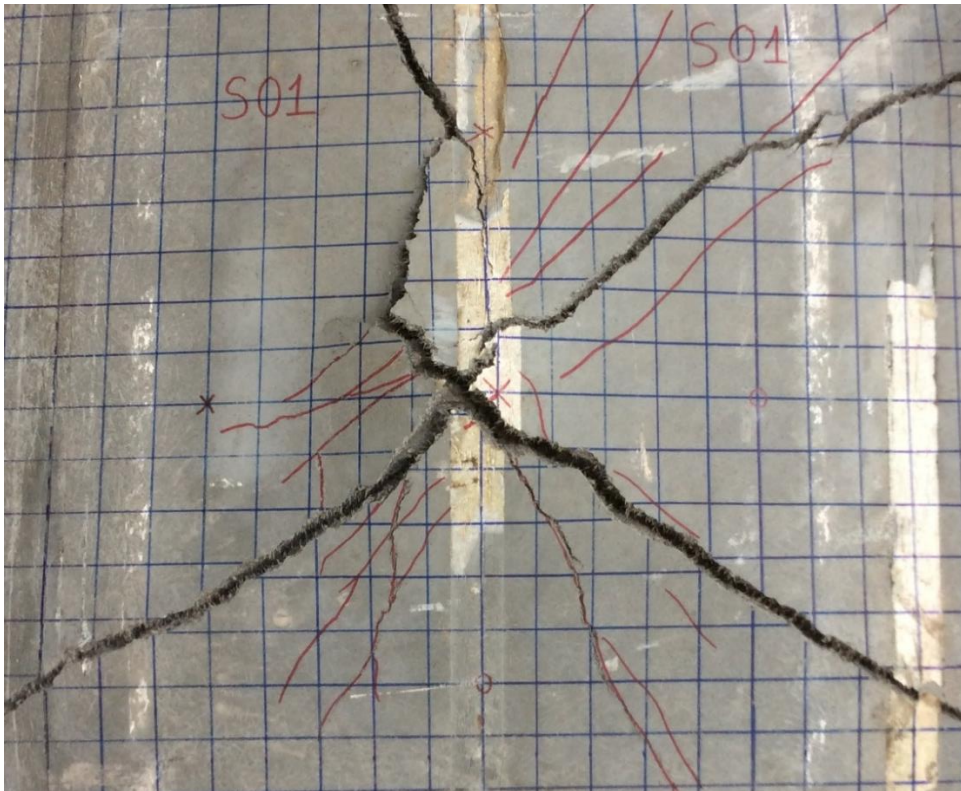
Figure 4.12 Tensile face of slab S01 failed in flexure

By increasing the steel fiber volume from 0.8 % to 1.6 %, the punching shear behavior changed from brittle behavior to more ductile behavior. Slabs with 1.6 % fibers showed fewer flexural cracks before critical shear crack opening. Slab S03 and S04 had the longitudinal cracks parallel to reinforcement which confirms the yielding of steel reinforcement near the loading area.

4.6 Fibers orientation and distribution

In order to obtain the steel fibers distribution and orientation in the concrete matrix, the UHPFRC slabs should be cut by half. The numbers of fibers and orientation were obtained by manual counting combining with image analysis techniques. Due to the time consuming of this method, in this study the fibers orientation and distribution were only investigated at some representative selection parts on the punching shear cone failure.

Figure 4.13 showed the typical fibers orientation of slab S02 when this slab was casted at the corner (position C). The two pieces were taken out from the punching cone. The fibers had a trend to align with an angle of 45°. It was clearly illustrated that the fibers had the similar orientation with the concrete flow direction.
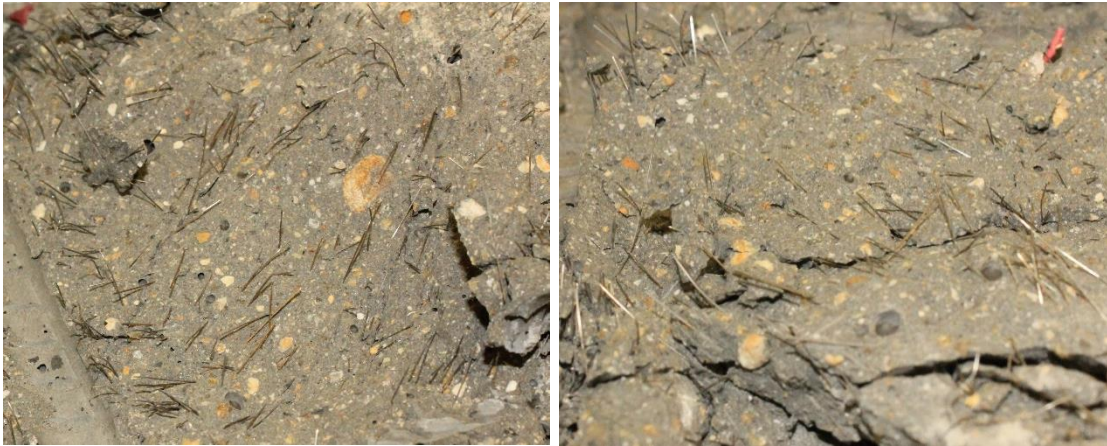
Figure 4.13 Fibers orientation when casting concrete at corner of the slab

For the slab S03 which was casted at one side of the slab, the fibers had a tendency of aligning along the concrete casting direction as can be seen in Figure 4.14. But for the part near the steel reinforcement, the fibers had a little change in the orientation. It could be explained by the effects of steel rebar in the casting procedure as mentioned in the previous section. When the concrete reached the rebar, the steel fibers orientation were suddenly changed. Figure 4.14 showed the typical orientation of steel fibers at two sections taken out from the punching cone failure.

For the last case, when the concrete was casted at the center position of the slab, the photos taken from the two pieces of the punching cone failure displayed the randomly distributed of the steel fibers in the concrete matrix. The fibers were aligned in all directions as can be seen in Figure 4.15.

Figure 4.14 Typical fibers orientation when casting concrete at one side of slab
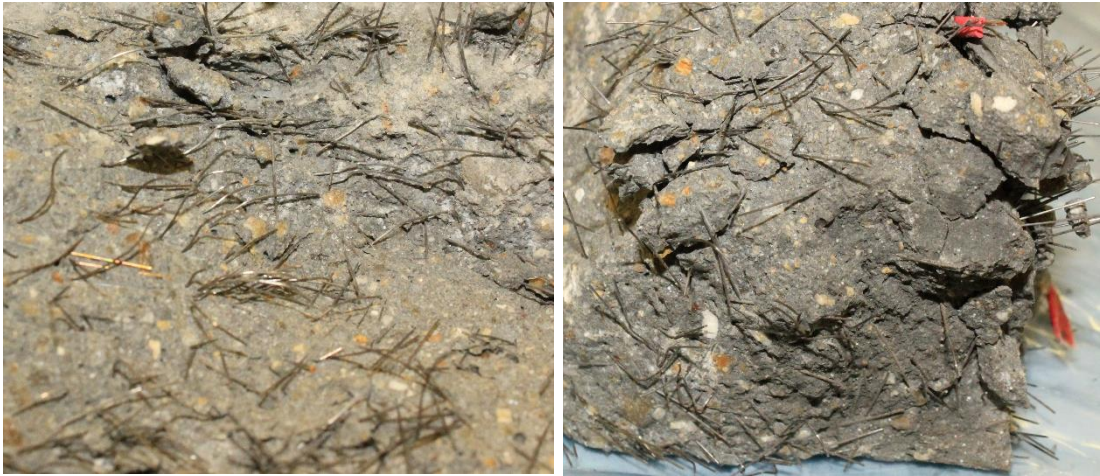
Figure 4.15 Fibers randomly distributed when casting at the center of the slab

For the slabs with high percentage of steel fibers (slabs S05, S06 and S07 with 1.6 % steel fiber) the fibers orientation were not considerably different between these slabs. While observing on the selected part, it was too difficult to visibly separate the preferred orientation of steel fibers in the matrix. A conclusion could be derived from the images analysis such that the fibers near the steel reinforcement distributed in a more random way than another positions. It might be explained by the blocking effect of rebar to fibers as mentioned in previous study.

4.7 Location of ultimate punching shear cone

In order to determine the positions of ultimate punching cone, an average distance of 8 points at the failure boundary on the tensile face evaluated from the center of the slab were applied [43] and then the angle of punching cone were sketched, as shown in Figure 4.16. The points were numbered from 1 to 8 clockwise and then the distance of each point was measured. The average distance was calculated and it was used to locate the position of ultimate punching cone for the tested slabs.

Figure 4.17 demonstrated the distance from the center to the location of the ultimate punching cone for each tested slab. From this figure, the slab S08 had the biggest distance from the center to the location of shear crack so that the punching shear cone was the largest one as presented above. The reason was due to the absence of steel fibers in the matrix so the steel reinforcement was early yielded and moved the shear cracks away from the load area.

In order to identify the effects of casting direction on the size of punching shear cone, the 6 slabs were divided by 2 group with the same fibers volume fraction but different in casting position such as: first group includes three slabs S02, S03 and S04; second group consists of three slabs S05, S06 and S07. In these two groups, the punching cone size obtained from the test showed clearly the effects of casting positions to each of slabs.
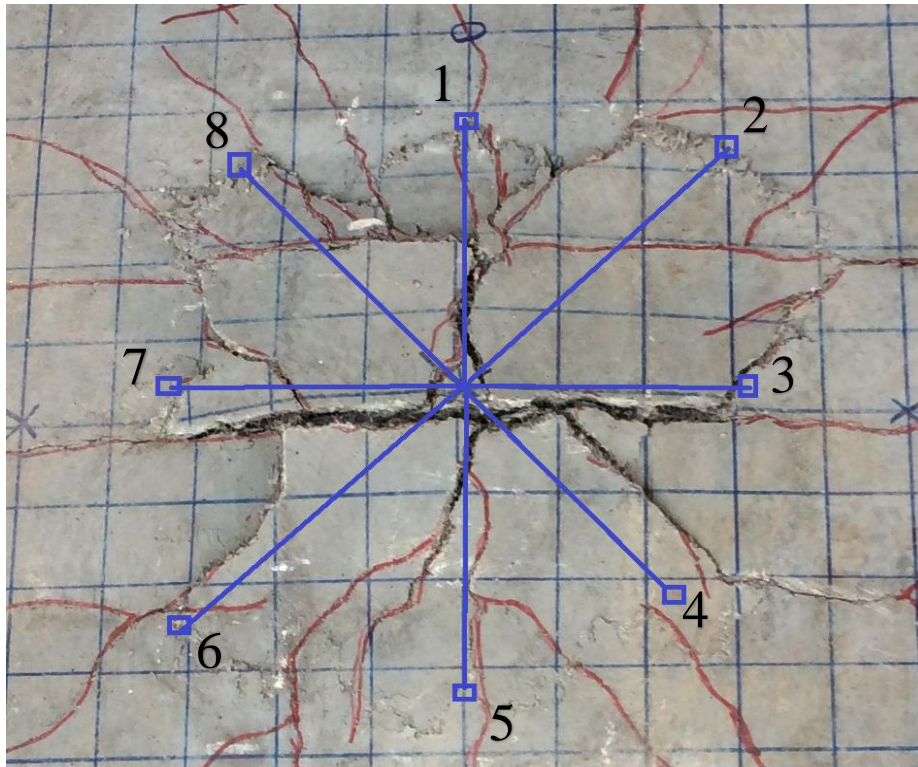
Figure 4.16 Method to measure the positions of shear cracks

For slabs S04 and S07 which were casted at the middle positions (position A), the punching shear cone were smaller while comparing with another slabs which were casted at position B and C. The reason for this may be explained by the random distribution of fibers. The fibers tried to orientate in all directions which much increased the resistance of the matrix and reduced the punching shear cone size as shown in Figure 4.17.

a)   b)
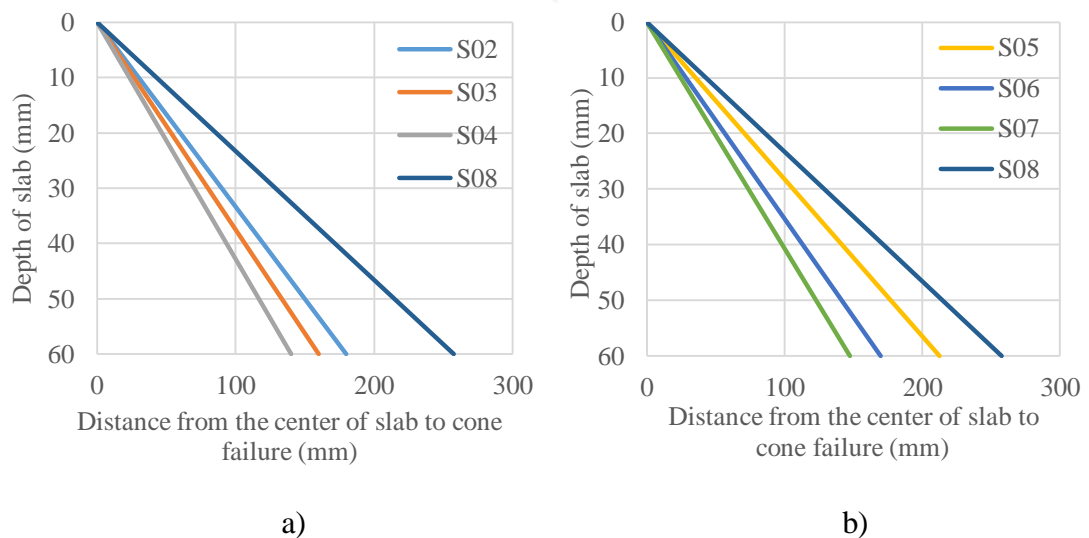
Figure 4.17 Location of ultimate punching shear cone

For slab S02 and S05 which were casted at position C, the punching shear cones were largest while comparing to another 2 group of slabs which indicated that the casting direction affected the punching shear cone size in some manner. The same conclusion were given with group of slabs S03 and S06 where the slabs were casted at one side of slabs. The fibers had the trend to align in only one direction matching with the concrete casting method. Then the punching cones were larger as the results.

The effects of casting direction on the size of punching shear cone were also specified while comparing each slab to others within 2 group of slabs: S02, S03, S04 and S05, S06, S07 which had the same fibers content but different in concrete casting direction. Slabs S04 and S07 which were casted at the middle of slabs showed the smaller punching cones while comparing to the slabs which were casted at another positions. Figure 4.17 clearly illustrated for this conclusion above.

Comparing with the punching shear cone size of other cases, the punching shear cone diameter of slabs S05, S06, S07 with steel reinforcement and highest steel fibers volume ratio (1.6 %) were expected to be smaller values but the experiment results showed that the size of punching cone were larger than that in slabs S02, S03 and S04 (with 0.8 % of steel fibers). It could be explained that the combination of steel reinforcement and fibers in S05, S06 and S07 showed the negative effects on the formation of punching shear cone due to the fibers blocking effects and 'wall-effect' that already mentioned in the previous section.

4.8 Fiber orientation factor

Due to the difference in casting method, the fiber orientation of the tested slabs were not similar as mentioned in the previous section. From the study of many researchers about FRC and UHPFRC, it could be concluded that the concrete flow had a huge effect in orientating the fiber orientation and the dispersion of steel fiber. In order to quantitative the fiber orientation number, the results from the study of Grunewald [22] about the relationship between fiber orientation and the distance from the concrete casting point were applied for this study.

The fiber orientation number was obtained by considering the distance from the concrete casting point to the ultimate punching shear cone failure position and comparing these values with the curves in Grunewald study which showed the relationship between fiber orientation number and distance from the casting point on four planes of the cone failure: two planes were perpendicular to the concrete flow direction and two planes were parallel to the wall surface. The average value of fiber orientation number was used for each slab in this study.

The distance from the center of the slab to the location of the ultimate punching shear perimeter was given in Figure 4.17 in the previous section. For the practical design, the position of ultimate failure cone was assumed to locate at the distance $2d$ from the loading path or column face as illustrated in Figure 4.18 as shown below.
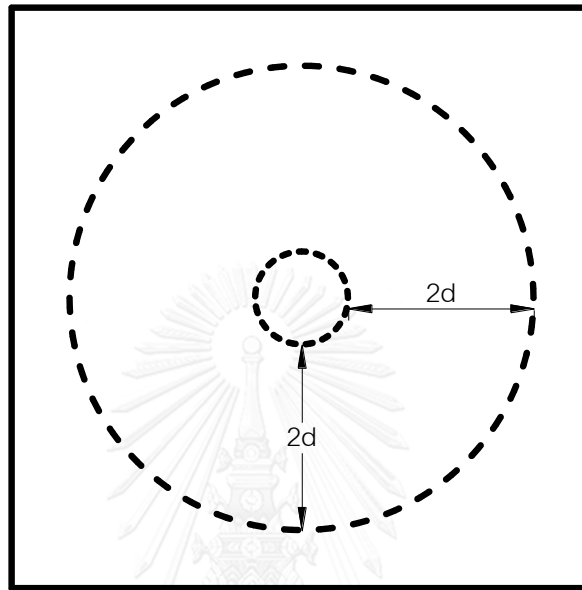
Figure 4.18 Proposed failure perimeter of tested slabs

The fiber orientation number was derived for 6 slabs in total of 8 tested slabs due to the slab S01 did not fail in punching shear mode and S08 did not contain any fibers within the concrete matrix. The results were summarized in Table 4.2 as below.

Table 4.2 Average fiber orientation number

Specimens	Average distance from the casting point to the failure surface (m)	Avg. fiber orientation number n_β
S02	2.31	0.618
S03	2.10	0.620
S04	0.20	0.615
S05	2.31	0.619
S06	2.10	0.621
S07	0.20	0.615

4.9 Proposed design equation

Based on the research of Narayanan and Darwish [17] about punching shear strength of steel fibers reinforced micro concrete slabs, a modified equation for predicting the punching shear capacity of UHPFRC slabs was proposed. Their experimental model was appropriate for this study since in their research, Narayanan and Darwish had supposed that no significant contribution of coarse aggregate (interlocking effect across the cracks) to resist shear force. It was suitable for the UHPFRC slabs in this test because this type of concrete did not contain any coarse aggregate in the mixing components.

There were many factors which affected to the punching shear strength of UHPFRC slabs. In their research, Narayanan and Darwish had considered three parameters which had a considerable contribution to the punching shear strength of steel fibers reinforced micro concrete slabs as:

- The concrete strength of the very narrow compressive zone above the top of the inclined cracks,

- The pull-out forces on the fibers along the inclined cracks, and

- The shear forces carried by the dowel and membrane actions.

Based on the same assumption, but using the results of the splitting tensile test and considering the global orientation factor to calculate the fibers factor, a new form of the present formula was proposed as follows:

$$v_{pre} = v_{pc} + v_{pf} + v_{pr} \tag{55}$$

where:

v_{pre} is the proposed punching shear strength of the UHPFRC slab;

v_{pc} is the shear resistance of very narrow compressive zone above the top of the inclined cracks;

v_{pf} is the pull-out forces on the fibers along the inclined cracks;

v_{pr} is the shear forces carried by tensile reinforcement;

In order to consider the dimension effect, a size factor ξ_s which depends on the depth of the slab was included. Combining the size factor ξ_s, splitting tensile strength obtained from the test and introducing the fiber orientation factor, the punching shear capacity can be calculated by the equation (56):

$$V_{pre} = \xi_s (v_{pc} + v_{pf} + v_{pr}) b_{of} d \tag{56}$$

with:

$$v_{pc} = 0.24 f_{spt} \tag{57}$$

$$v_{pf} = 0.41 \tau F \tag{58}$$

$$v_{pr} = 16 \rho \tag{59}$$

$$\xi_s = 1.6 - 0.002h \tag{60}$$

$$F = \frac{L}{D} V_f d_f n_f \tag{61}$$

$$b_{of} = (b_0 + 4\pi d)(1 - KF) \tag{62}$$

where:

f_{spt} is the tensile strength derived from the splitting tensile test, MPa

τ is average fiber matrix interfacial bond stress, $\tau = 4.15$ MPa

ρ is average tension steel reinforcement ratio

h is the overall depth of slab, mm

F is the fiber factor

b_o is perimeter of loading pad or column, mm

b_{of} is perimeter of the critical section located at a distance of $2d$ from the edge of the loading pad or column face, mm

L is the length of fiber, mm

D is the diameter of fiber, mm

V_f is fiber volume ratio

d_f is the bond factor, taken as 0.5 for round fiber, 0.75 for crimped fiber and 1.0 for hooked-ends fiber

n_β is the fiber orientation factor, as given in Table 10

d is the effective depth of the slab

K is the non-dimensional constant value ($K = 0.54$)

ξ_s is the empirical depth factor

The proposed equation (56) was applied for the 7 tested slabs in this study to calculate the prediction punching shear strength and then comparing the predicted results with the test results due to slab S01 failed in flexural mode. The calculation were detailed and summarized in Table 4.3 as below.

Table 4.3 Punching predicted values with fiber orientation number

| Slab | Tensile reinforcement | | | Fibers | | | f_{spt} (MPa) | b_{of} (mm) | V_{test} (kN) | V_{pre} (kN) | $\dfrac{V_{test}}{V_{pre}}$ |
	Thickness	Effective depth (mm)	Ratio ρ (%)	Ratio V_f (%)	F	n_β					
S02	60	40	2.54	0.80	0.16	0.618	8.2	688	121.9	108.00	1.13
S03	60	40	2.54	0.80	0.16	0.620	8.6	688	108.3	111.50	0.97
S04	60	40	2.54	0.80	0.16	0.615	7.6	688	125.8	101.82	1.24
S05	60	40	2.54	1.60	0.32	0.619	12.1	622	147.6	141.97	1.04
S06	60	40	2.54	1.60	0.32	0.621	11.7	622	168.9	138.37	1.22
S07	60	40	2.54	1.60	0.32	0.615	11.8	623	143.0	139.31	1.03
S08	60	40	2.54	0.00	0.00	0.000	5.4	754	87.3	76.46	1.14
										Avg.	1.109
										S.D	0.101

In order to investigate the effects of fiber orientation number to fiber factor and also to predicted value of punching shear failure, the calculation of this value without fiber orientation number was conducted and it was shown in Table 4.4 as below. The outcomes showed that the obtained results were more accurate with the consideration of the fiber orientation number. The average ratio between the test and predicted value

with and without fiber orientation number decreased from 1.135 to 1.109 with the standard deviation around 0.101 and 0.102, respectively.

Table 4.4 Punching predicted values without fiber orientation number

| Slab | Tensile reinforcement | | | Fibers | | f_{spt} (MPa) | b_{of} (mm) | V_{test} (kN) | V_{pre} (kN) | $\dfrac{V_{test}}{V_{pre}}$ |
	Thickness	Effective depth (mm)	Ratio ρ (%)	Ratio V_f (%)	F					
S02	60	40	2.54	0.80	0.26	8.2	647	121.9	108.09	1.13
S03	60	40	2.54	0.80	0.26	8.6	647	108.3	111.38	0.97
S04	60	40	2.54	0.80	0.26	7.6	647	125.8	102.28	1.23
S05	60	40	2.54	1.60	0.52	12.1	541	147.6	134.23	1.10
S06	60	40	2.54	1.60	0.52	11.7	541	168.9	131.12	1.29
S07	60	40	2.54	1.60	0.52	11.8	541	143.0	131.86	1.08
S08	60	40	2.54	0.00	0.00	5.4	754	87.3	76.46	1.14
									Avg.	1.135
									S.D	0.102

In order to consider the contribution of each component on the total punching shear strength of UHPFRC slabs, the comparison between the contribution of v_{pc}, v_{pf}, v_{pr} to the total punching shear strength of each slabs were summarized in the Table 4.5 as shown below.

Table 4.5 Contribution of each components to the punching shear strength

| Slab | V_{pc} | | V_{pf} | | V_{pr} | | V_{pre} (kN) |
	Calculated value (kN)	Contribution to predicted value (%)	Calculated value (N/mm2)	Contribution to predicted value (%)	Calculated value (N/mm2)	Contribution to predicted value (%)	
S02	54.24	74.33	7.53	10.31	11.21	15.36	108.00
S03	56.59	75.11	7.55	10.02	11.20	14.87	111.50
S04	50.10	72.81	7.49	10.89	11.21	16.30	101.82
S05	72.17	75.23	13.63	14.21	10.13	10.56	141.97
S06	69.71	74.56	13.66	14.61	10.12	10.83	138.37
S07	70.43	74.82	13.56	14.40	10.14	10.78	139.31
S08	39.38	76.23	0.00	0.00	12.28	23.77	76.46

From the results presented in Table 4.5, the part which was most contributed to the predicted value of punching shear strength was the concrete contribution which was around 75 % in average. The steel fiber contribution was less than 15 % while the reinforcement contribution was less than 16 % for almost slabs (excluding slab S08 without fiber). It could be concluded that the strength of concrete (maximum tensile strength in this study) much affected to the punching shear strength of UHPFRC slabs whereas the contribution of steel fiber and steel reinforcement were not considerably recognized. Due to this reason, the fiber orientation number mentioned in the previous section was not significantly influenced to the total punching shear failure strength.
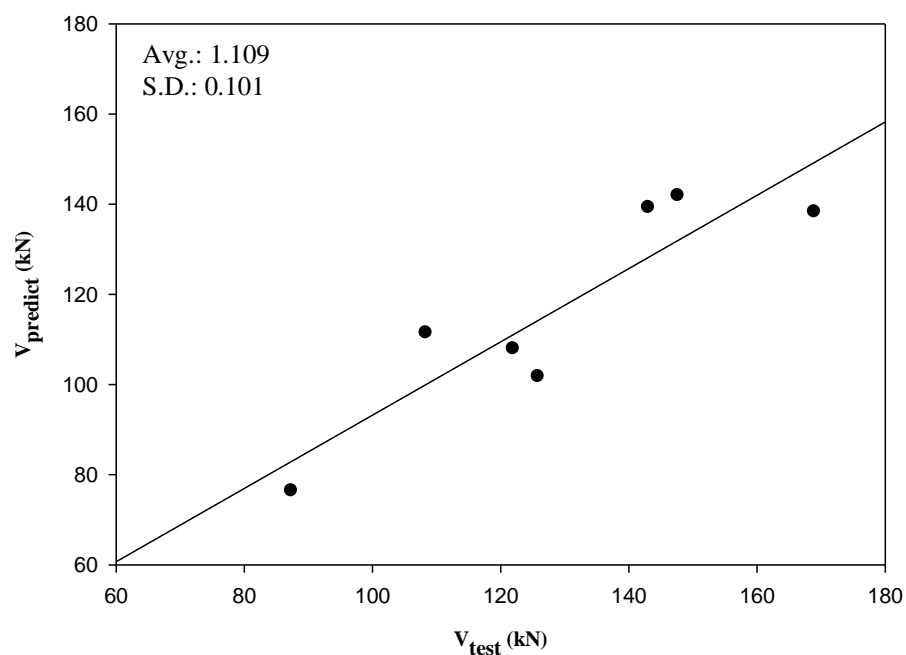
Figure 4.19 Comparison test value and predicted value

In order to determine the accuracy of the proposed equation, the test results and the predicted results given by equation (56) were compared. This comparison was plotted in Figure 4.20. It was observed that the results of the proposed design equation agreed well with the test results conducted on the UHPFRC slabs in this study. The mean value of the ratios (the test values to the predicted values) was 1.101 with a standard deviation of 0.076. Then the proposed design equation can predict the punching shear strength of UHPFRC slabs with and without fibers with an applicable accuracy.

CHAPTER 5

CONCLUSIONS AND RECOMMENDATIONS

5.1 Conclusions

The studies conducted during this experimental work have given a better understanding of the punching shear behavior of the UHPFRC slabs. In this study, UHPFRC was considered as an advanced cementitious materials. It can be used in structural elements which require high strength, ductility and long term durability. The objectives of this research was to determine the effects of casting direction on punching shear strength of UHPFRC slabs and proposed a modified equation to predict the punching shear capacity taking into account the fiber orientation and splitting tensile capacity of UHPFRC.

The total eight square slabs with a dimension of 1000 mm in both side had been tested to investigate the punching shear strength and the behavior of these slabs at the ultimate failure load. The varying parameters among these specimens were the fibers volume ratio from 0 to 1.6 % and fibers orientation due to the difference in casting position. The test results from the punching shear test showed that when increasing steel fiber from 0 to 0.8 % and 1.6 %, the failure load increased as well from 87 kN to 125 kN and 168 kN, equivalent to 43 % and 93 %, respectively. Fibers also changed the failure modes of the UHPFRC slabs. The slab without fibers failed at the lower load than slabs with fibers. Moreover, the slabs without fibers showed the brittle failure behavior with the splitting of the concrete cover and might be the reason to limit tensile strength of concrete.

Adding fibers to the concrete mixture can also delay the appearance of first cracks. According to the test results, when the steel fibers content increased from 0 to 0.8 % and 1.6 %, the first cracking load significantly increased from 18 kN to 27 kN and 36 kN, corresponding to 46 % and 96 %, respectively. When comparing between 0.8 % and 1.6 % of steel fibers, the first cracking load rose an amount equivalent to 34 %. The failure load of the slab with tensile reinforcement but without fibers was closed to that value on the slab without tensile reinforcement but with 1.6 % of steel fibers. It can be concluded that the steel fibers had the same capacity to resist the load as the tensile reinforcement.

For the tested slabs, two types of failure modes were demonstrated. The slab without tensile reinforcement failed in flexural mode, characterized by the diagonal cracks from the center to the end of the slab. For the slabs with tensile reinforcement, the failure mode were punching shear, characterized by the appearance of the punching cone at the ultimate failure load. The slab with tensile reinforcement but without fibers failed in punching shear modes and created a big punching cone compared to the slabs with steel fibers.

The effects of casting position on punching shear of tested slabs were illustrated based on the size of failure cone. The slabs which were casted at the center of formwork showed the smallest punching cone size while comparing to the slabs which were casted at the corner or along one side of the mold. It could be explain by the fibers had a trend

to randomly distribute and orient in all direction in the concrete matrix which might help the matrix to resist forces in all directions, increased the failure load and reduced the punching cone size as a result. The slabs casted at the corner or along one side presented the bigger punching cone might be explained by the fibers tended to align in one direction matching the concrete flow direction. The slabs with 1.6 % of steel fibers were expected to have the smaller critical shear perimeter while comparing to slabs with 0.8 %, however the results from the test showed the contradictory trend, the punching cone size were not less than or even larger. It might be clarified by the negative effects due to fibers blocking phenomenon and wall effects.

The fibers orientation number was one of the factors which contributed to the fiber factor and punching shear capacity of UHPFRC slabs. The proposed equation considered the fibers orientation, maximum tensile strength derived from the splitting tensile test and the modified critical shear perimeter gave the good prediction of the punching shear capacity of UHPFRC slabs without or with straight steel fibers with an applicable accuracy. The average value of the ratios between the test values and the predicted values was 1.109 with a standard deviation of 0.101.

5.2 Recommendations

For the future study, it is recommended to:

- Study the effects of tensile reinforcement ratio and type of steel fibers on punching shear behavior. The bond behavior between the fibers and concrete matrix, influence of tensile reinforcement on fibers orientation should be investigate.

- In this study only axisymmetric punching shear capacity was inspected. The study of nonsymmetrical punching shear strength of UHPFRC slabs is also necessary.

- Further investigation of the proposed equation for predicting the punching shear strength of UHPFRC slabs should be conducted. The experiment data from the other researches should be used to verify the accuracy of the proposed equation and compare with the other equations.

- Modelling of the UHPFRC slabs should be performed in order to compare the test results and finite element analysis by using simulation software.

REFERENCES

1]. Committee, A. Building Code Requirements for Structural Concrete (ACI 318-11) and Commentary. in American Concrete Institute. 2011.

[2]. EN 1992-1-1, E., Design of concrete structures, in Part 1-1: General rules and rules for buildings. 2004.

[3]. JSCE, Recommendations for Design and Construction of High Performance Fiber Reinforced Cement Composites with Multiple Fine Crack (HPFRCC). 2008, Japan Society Of Civil Engineers.

[4]. AFGC-SETRA, Ultra High Performance Fiber Reinforced Concrete Recommendations. 2013, French Association for Civil Engineers (AFGC).

[5]. Search, G. Some popular kinds of fibers on the global construction market. 2000; Available from: http://3.imimg.com/data3/QE/AT/MY-2203460/hook-end-steel-fiber-250x250.jpg,
http://i01.i.aliimg.com/photo/v0/202882681/Cement_based_Concrete_Polypropylene_Fiber.jpg, http://texnoteblog.files.wordpress.com/2014/01/e7929-product5.jpg, .

[6]. Van Tuan, N., et al., Hydration and microstructure of ultra high performance concrete incorporating rice husk ash. Cement and Concrete Research, 2011. 41(11): p. 1104-1111.

[7]. Yang, S., et al., Influence of aggregate and curing regime on the mechanical properties of ultra-high performance fibre reinforced concrete (UHPFRC). Construction and Building Materials, 2009. 23(6): p. 2291-2298.

[8]. Yu, Q., P. Spiesz, and H. Brouwers, Development of cement-based lightweight composites–Part 1: Mix design methodology and hardened properties. Cement and Concrete Composites, 2013. 44: p. 17-29.

[9]. Spasojevic, A., et al. Influence of tensile properties of UHPFRC on size effect in bending. in Ultra High Performance Concrete (UHPC), Second International Symposium on Ultra High Performance Concrete. 2008. Ultra High Performance Concrete (UHPC), Second International Symposium on Ultra High Performance Concrete.

[10]. Naaman, A. Toughness, ductility, surface energy and deflection-hardening FRC composites. in Proceedings of the JCI Workshop on Ductile Fiber Reinforced Cementitious Composites (DFRCC)–Application and Evaluation, Japan Concrete Institute, Tokyo, Japan. 2002.

[11]. Structural Group, R.M., Punching shear failure in a 4-story, concrete flat slab construction, commercial parking garage, Christchurch CBD, New Zealand., C.e.r.p.T.f. days, Editor. 2011.

[12]. Kinnunen, S. and H. Nylander, Punching of concrete slabs without shear reinforcement. 1960: Elander.

[13]. Muttoni, A., Shear and punching strength of slabs without shear reinforcement. Beton- und Stahlbetonbau, 2003. 98(2): p. 74-84.

[14]. Muttoni, A., Punching shear strength of reinforced concrete slabs without transverse reinforcement. ACI Structural Journal, 2008. 105(EPFL-ARTICLE-116123): p. 440-450.

[15]. Muttoni, A. and M. Fernández Ruiz, MC2010: The Critical Shear Crack Theory as a mechanical model for punching shear design and its application to code provisions. fib Bulletin, 2010. 57.

[16]. Muttoni, A. and J. Schwartz. Behaviour of beams and punching in slabs without shear reinforcement. in IABSE Colloquium. 1991. IABSE Colloquium.

[17]. Narayanan, R. and I. Darwish, Punching shear tests on steel-fibre-reinforced micro-concrete slabs. Magazine of Concrete Research, 1987. 39(138): p. 42-50.

[18]. Tan, K.-H. and P. Paramasivam, Punching shear strength of steel fiber reinforced concrete slabs. Journal of materials in civil engineering, 1994. 6(2): p. 240-253.

[19]. Harajli, M., D. Maalouf, and H. Khatib, Effect of fibers on the punching shear strength of slab-column connections. cement and concrete composites, 1995. 17(2): p. 161-170.

[20]. Higashiyama, H., A. Ota, and M. Mizukoshi, Design equation for punching shear capacity of SFRC slabs. International Journal of Concrete Structures and Materials, 2011. 5(1): p. 35-42.

[21]. Narayanan, R. and A. Kareem-Palanjian, Effect of fibre addition on concrete strengths. Indian Concrete Journal, 1984. 58(4): p. 100-103.

[22]. Grünewald, S., Performance-based design of self-compacting fibre reinforced concrete. 2004: Delft University Press Delft, The Netherlands.

[23]. Pansuk, W., et al. Tensile behaviors and fiber orientation of UHPC. in Proceedings of second international symposium on ultra high performance concrete, Kassel, Germany. 2008.

[24]. Kim, S.W., et al. Effect of filling method on fibre orientation & dispersion and mechanical properties of UHPC. in Proceedings of second international symposium on ultra high performance concrete, Kassel, Germany. 2008.

[25]. Kooiman, A.G., Modelling steel fibre reinforced concrete for structural design. 2000: TU Delft, Delft University of Technology.

[26]. Martinie, L. and N. Roussel, Simple tools for fiber orientation prediction in industrial practice. Cement and Concrete research, 2011. 41(10): p. 993-1000.

[27]. Barnett, S.J., et al., Assessment of fibre orientation in ultra high performance fibre reinforced concrete and its effect on flexural strength. Materials and structures, 2010. 43(7): p. 1009-1023.

[28]. Markovic, I., High-performance hybrid-fibre concrete: development and utilisation. 2006: IOS Press.

[29]. Álvarez, A.B., Characterization and modelling of SFRC elements. 2013, Polytechnique of Barcelona.

[30]. Kang, S.-T. and J.-K. Kim, The relation between fiber orientation and tensile behavior in an Ultra High Performance Fiber Reinforced Cementitious Composites (UHPFRCC). Cement and Concrete Research, 2011. 41(10): p. 1001-1014.

[31]. Kang, S.-T. and J.-K. Kim, Investigation on the flexural behavior of UHPCC considering the effect of fiber orientation distribution. Construction and Building Materials, 2012. 28(1): p. 57-65.

[32]. Stroeven, P. and S. Shah, Use of radiography-image analysis for steel fiber reinforced concrete. Testing and Test Methods of Fiber Cement Composites, 1978: p. 345-353.

[33]. Attachaiyawuth, A., Experimental crack-shear slip model for high strength concrete reinforced with steel fiber by direct shear-push off test, in Department of Civil Engineering. 2011, Chulalongkorn University.

[34]. Lionel Moreillon, R., Shear and punching shear behaviour of structural elements in High Performance Fibre Reinforced Concrete 2013, Université Paris-Est.

[35]. Materials, A.S.f.T.a., ASTM C 150, 2007. Standard Specification for Portland Cement.

[36]. Tests, C.-S., ASTM C 39/C 39M; test one set of two laboratory-cured specimens at 7 days and one set of two specimens at 28 days. a. Test one set of two field-cured specimens at. 7.

[37]. Materials, A.S.f.T.a., ASTM 496/C 496M, in Standard test method for splitting tensile strength of cylindrical concrete, ASTM, West Conshohocken, PA. 2011. p. 5.

[38]. Ma, J., et al. Comparative investigations on ultra-high performance concrete with and without coarse aggregates. in Proceedings International Symposium on Ultra High Performance Concrete (UHPC), Kassel, Germany. 2004.

[39]. Graybeal, B.A., Compressive behavior of ultra-high-performance fiber-reinforced concrete. ACI Materials Journal, 2007. 104(2).

[40]. 363, A.C. State of the Art Report on High-Strength Concrete (ACI 363R-92). in ACI Journal Proceedings. 1992. ACI.

[41]. Materials, A.S.f.T.a., ASTM C 469, in Standard test method for static modulus of elasticity and Poisson's ratio of concrete in compression. 2001.

[42]. Lee, N. and D. Chisholm, Study report reactive powder concrete. BRANZ, 2005. 1(1): p. 146.

[43]. Al-Quraishi, H.A.A., Punching Shear Behavior of UHPC Flat Slabs, in Faculty of Civil and Environmental Engineering. 2014, University of Kassel: Institute of Structural Engineering.
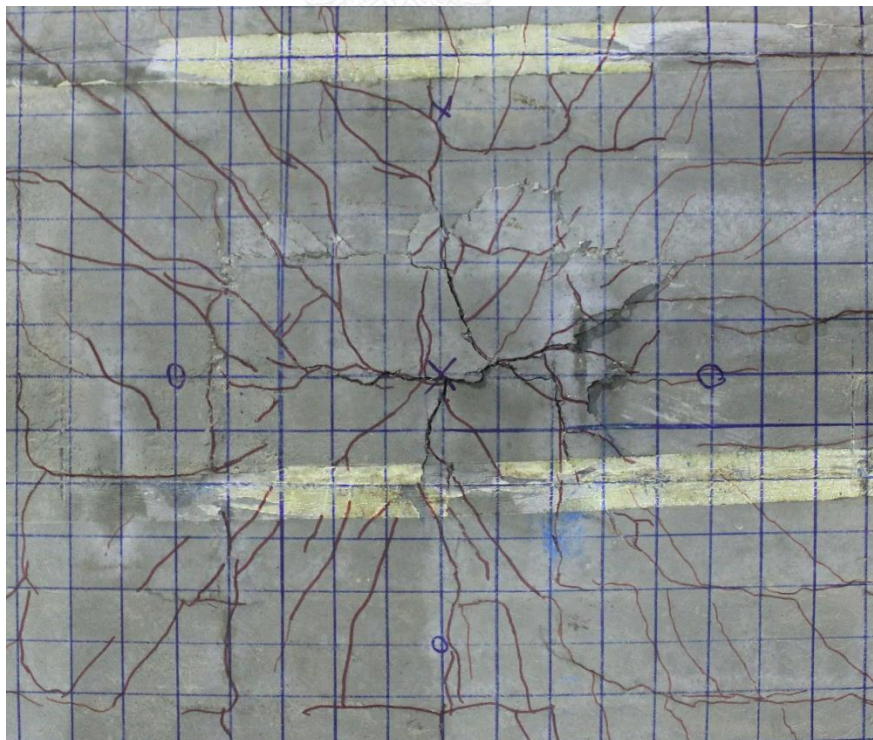
APPENDIX

Crack pattern and failure surface of the tested slab
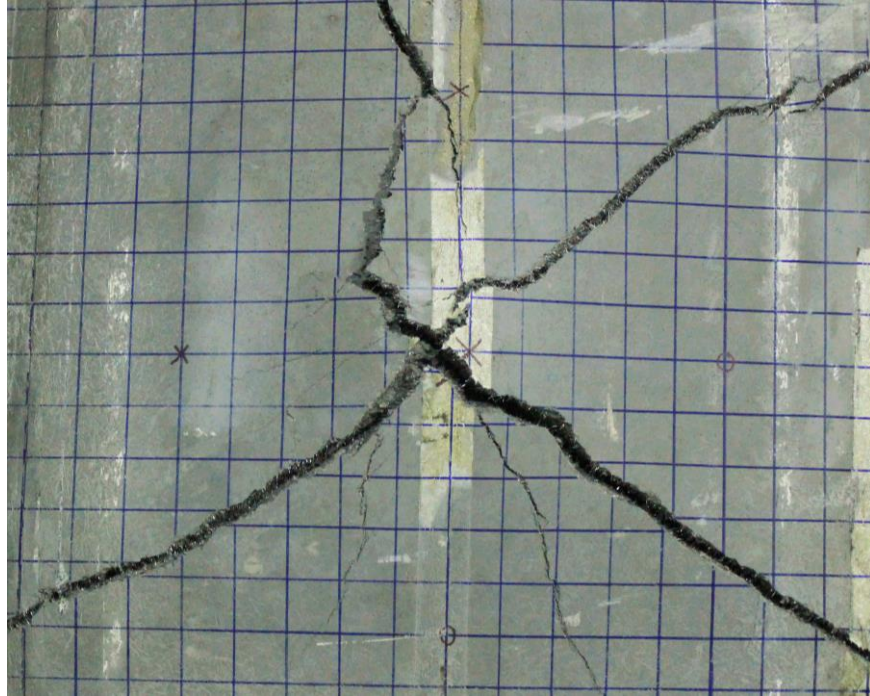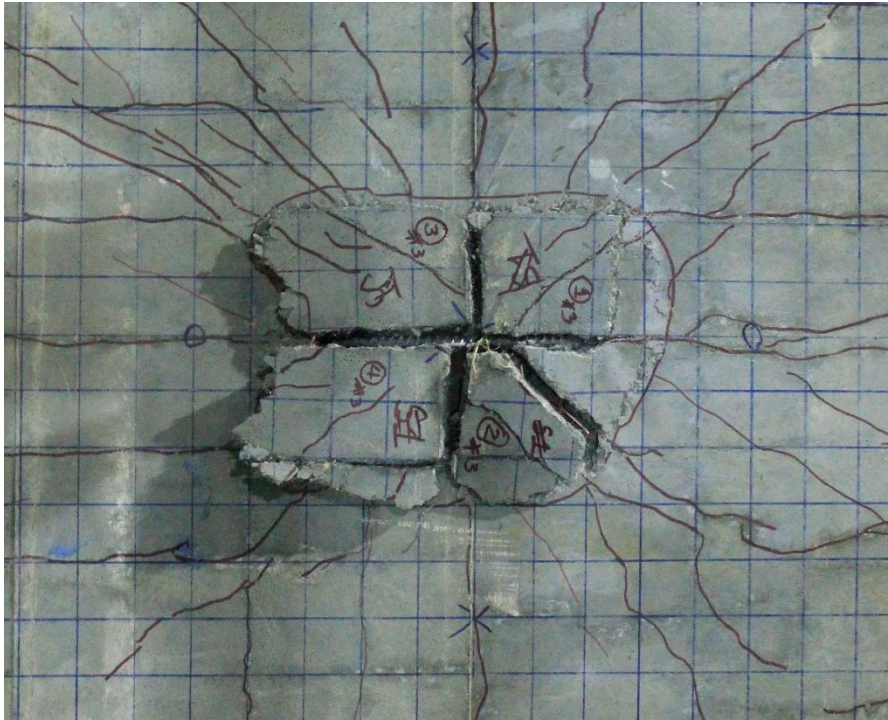

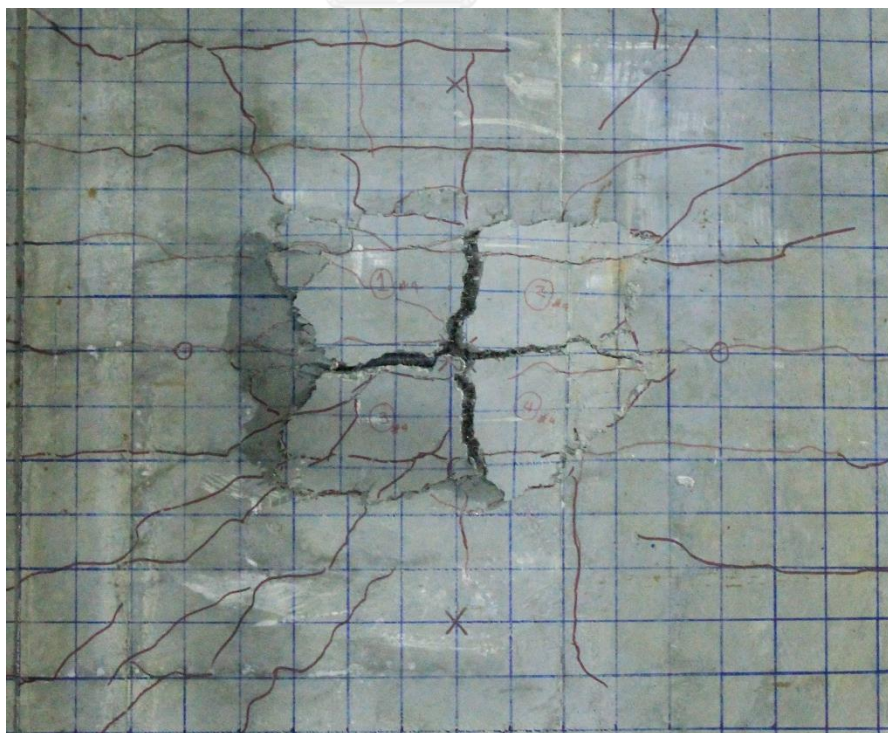**Fig A1 - Failure surface of the slab S01**

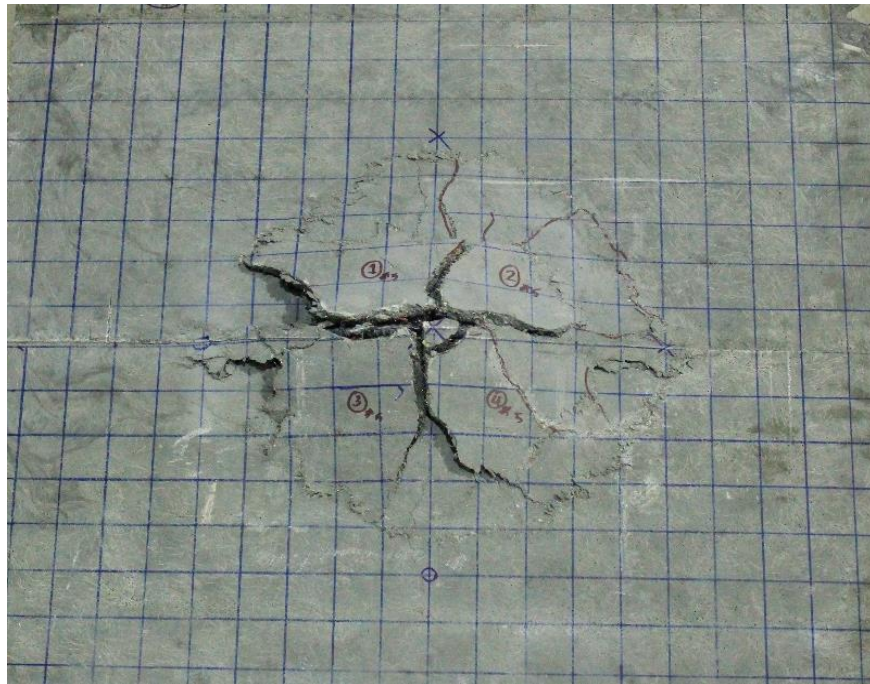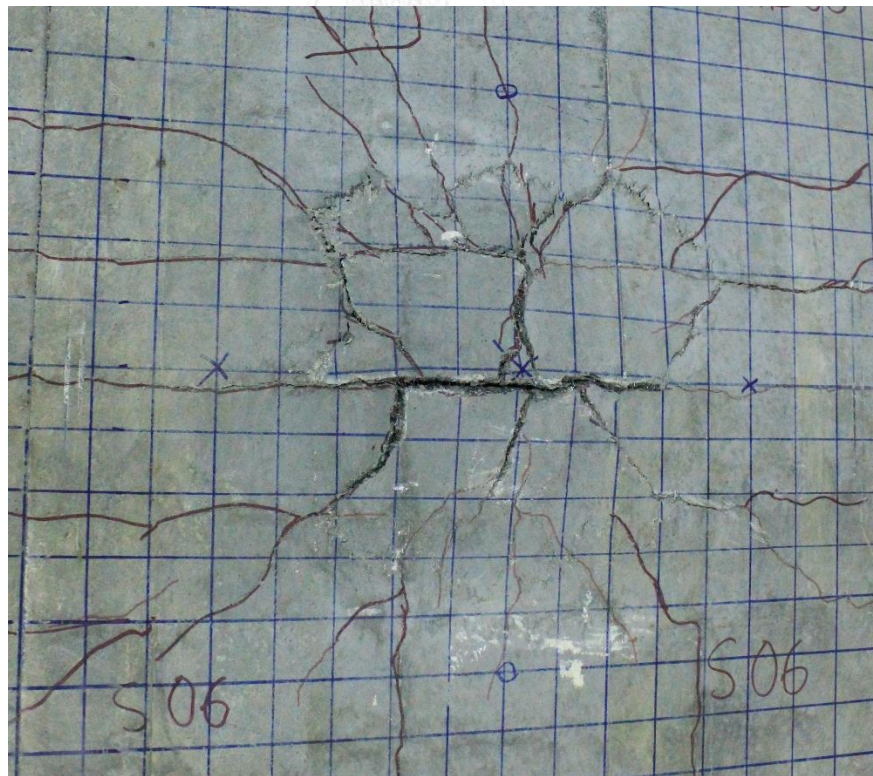**Fig A2 - Failure surface of the slab S02**

Fig A3 - Failure surface of the slab S03

Fig A4 - Failure surface of the slab S04

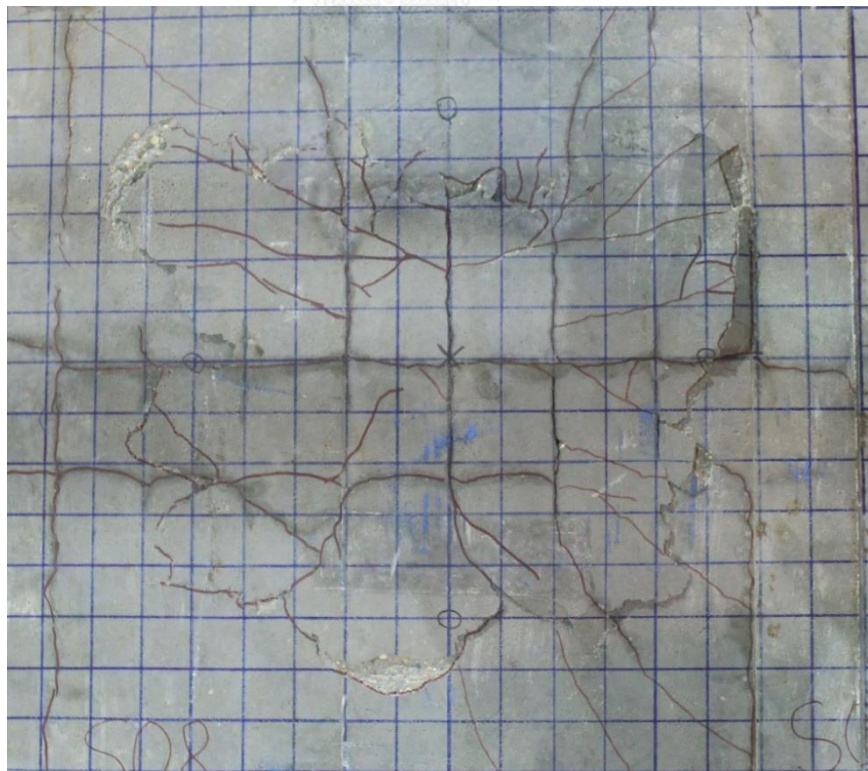**Fig A5 - Failure surface of the slab S05**

Fig A6 - Failure surface of the slab S06

Fig A7 - Failure surface of the slab S07

Fig A8 - Failure surface of the slab S08

VITA

Name: Mr. Tung Nguyen Thanh

Date of birth: October 02, 1988

Education:

2006-2011 Bachelor's degree in Hydraulic Engineering, Water Resources University 2nd Base, Ho Chi Minh city, Vietnam.

2013-2015 Master's degree student in Structural Engineering, Faculty of Engineering, Chulalongkorn University, Bangkok, Thailand.

Publications:

T. N. Thanh and W. Pansuk (2015). Effects of casting direction on punching shear strength of Ultra High Performance Steel Fiber Reinforced Concrete. Paper presented at the 20th National Convention on Civil engineering, 8-10 July 2015, Pattaya, Chonburi, Thailand.